

AN ELASTIC –PLASTIC BEAM FINITE ELEMENT

A THESIS SUBMITTED TO
THE GRADUATE SCHOOL OF NATURAL AND APPLIED SCIENCES
OF
MIDDLE EAST TECHNICAL UNIVERSITY

BY

AHMET M. EREN

IN PARTIAL FULFILLMENT OF THE REQUIREMENTS
FOR THE DEGREE OF MASTER OF SCIENCE

IN

MECHANICAL ENGINEERING

APRIL 2006

Approval of the Graduate School of Natural and Applied Sciences

Prof. Dr. Canan ÖZGEN

Director

I certify that this thesis satisfies all the requirements as a thesis for the degree of Master of Science.

Prof. Dr. Kemal İDER

Head of Department

This is to certify that we have read this thesis and that in our opinion it is fully adequate ,in scope and quality, as a thesis for the degree of Master of Science.

Prof. Dr. Kemal İDER

Co-Supervisor

Examining Committee Members

Assoc.Prof. Dr. Suat KADIOĞLU (ME/METU) _____

(Chairman)

Prof. Dr. Haluk DARENDELİLER(ME/METU) _____

(Supervisor)

Prof. Dr. Kemal İDER (ME/METU) _____

(Co-Supervisor)

Prof. Dr. Yavuz YAMAN (AEE/METU) _____

Asst. Prof. Dr. Serkan DAĞ (ME/METU) _____

I hereby declare that all information in this document has been obtained and presented in accordance with academic rules and ethical conduct. I also declare that, as required by these rules and conduct, I have fully cited and referenced all material and results that are not original to this work.

Name, Last name : Ahmet M. EREN

Signature :

ABSTRACT

AN ELASTIC-PLASTIC BEAM ELEMENT

EREN, Ahmet M.

M. Sc. Department of Mechanical Engineering

Supervisor: Prof. Dr. Haluk DARENDELİLER

Co-Supervisor: Prof. Dr. Kemal İDER

April 2006, 85 pages

In this thesis, a two node nonlinear elastic-plastic beam finite element is developed to analyze large deformations. The system of equations are derived from virtual work principle, and the updated Lagrangian formulation is used. Material is assumed to be isotropic and rate insensitive obeying J_2 -flow rule. Work hardening characteristics of material is considered and all nonlinear terms are included. For the two node iso-parametric beam element a layered model is used to analyze through-the-thickness distribution of elastic and plastic zones. A finite element program is developed and the numerical outcomes are compared with the experimental results. A good agreement is achieved between numerical and experimental results.

Keywords: Finite Element Method, Beam Finite Element, Elastic-Plastic Deformation

ÖZ

ELASTİK-PLASTİK BİR KİRİŞ SONLU ELEMAN

EREN, Ahmet M.

Yüksek Lisans , Makine Mühendisliği Bölümü

Tez Yöneticisi: Prof. Dr. Haluk DARENDELİLER

Ortak Tez Yöneticisi: Prof. Dr. Kemal İDER

Nisan 2006, 85 sayfa

Bu tezde büyük elastik-plastik şekil değiştirmelerin analizi için bir kiriş sonlu elemanı geliştirilmiştir. Sistem denklemleri virtuel iş prensibi ve yenilemeli Lagrange formülasyonu kullanılarak elde edilmiştir. Malzemenin izotropik ve hız değişikliklerine duyarız olduğu varsayılmış ve lineer olmayan bütün terimler formülasyona dahil edilmiştir. İki düğüm noktalı eşparametrik kiriş sonlu elemanı için kalınlık boyunca katmanlı bir yapı kullanılarak elastik ve plastik bölgeler belirlenmiştir. Bu amaçla bir sonlu eleman yazılımı geliştirilmiş ve sayısal çıktılar deneysel sonuçlarla kıyaslanmıştır. Sayısal ve deneysel sonuçlar arasında iyi bir uyum olduğu görülmüştür.

Anahtar Kelimeler: Sonlu Elemanlar Yöntemi, Kiriş Sonlu Elemanı,
Elastik –Plastik Şekil Değiştirme

ACKNOWLEDGEMENTS

I would like to express my sincere appreciation to Prof. Dr. Haluk DARENDELİLER and Prof. Dr. Kemal İDER for their guidance through the thesis work.

TABLE OF CONTENTS

PLAGIARISM	iii
ABSTRACT.....	iv
ÖZ.....	v
ACKNOWLEDGEMENTS.....	vi
TABLE OF CONTENTS.....	vii
LIST OF FIGURES.....	ix
CHAPTER	
1. INTRODUCTION.....	1
2. LITERATURE SURVEY.....	3
2.1 Previous Studies.....	3
2.2 Present Study.....	15
3. FORMULATION and GOVERNING EQUATIONS	
3.1 Virtual Work Principle	16
3.2 Virtual Work Formulation of Nodal Variables.....	28
3.2.1 Displacement Field of Timoshenko Beam.....	28
3.2.2 Two Dimensional Beam Element	29
3.3 Constitutive relation.....	37
3.4 Global Stiffness Matrix.....	39
3.5 The Newton-Raphson Method.....	40
3.6 Convergence Criteria.....	42
3.7 The Solution Procedures.....	44
3.8 Algorithm for the Finite Element Code.....	45
4. RESULTS and DISCUSSION.....	48
4.1 Case I : Specimen Clamped from One Side.....	48

4.2 Case II: Specimen Clamped from One Side	61
4.3 Discussion of the Results.....	70
5. CONCLUSION	72
REFERENCES.....	74
APPENDICES	
A. FLOWCHART OF THE PROGRAM.....	82
B. STRESS-STRAIN CURVE OF THE SPECIMEN.....	85

LIST OF FIGURES

FIGURE

3.1 An Infinitesimal Body Deformed and Undeformed Configuration.....	17
3.2 3D Beam Element Nodal Variables.....	28
3.3 Two Dimensional Beam Element Nodal Variables.....	29
3.4 The Iso-parametric Beam Element.....	31
4.1 The Loading and Boundary Conditions for Specimen Clamped from One End.....	49
4.2 Deflections Obtained from Experiments and Finite Elements for a 2,68 mm Specimen Clamped from On Side Under the Loads a)35N, b)40 N, c)45 N, d)50 N	50

4.3 Elements Deformed Plastically at a) 40 mm b) 50 mm c) 60 mm d) 70 mm e) 80 mm f) 90 mm g) 100 mm h) 110mm i) 120 mm j) 130 mm k)140 mm l) 150 mm m) 160 mm n) 165 mm.....	54
4.4 The Loading Geometry and Boundary Conditions for Specimen Clamped from Two Ends.....	61
4.5 Deflections Obtained for a Test Specimen Clamped from Two Sides Under the Loads a) 50N b)100 N c)150 N d)200 N.....	62
4.6 Elements Deformed Plastically at a) 3.5 mm b) 4 mm c) 4.5 mm d) 5 mm e) 5.5 mm f) 6 mm g) 6.5 mm h) 7 mm.....	66
B.1 The Stress-Strain Curve of the 2,68 mm Test Specimen.....	85

CHAPTER I

INTRODUCTION

An elastic-plastic beam element for large strain and large displacement analysis is developed in this thesis.

Many researchers have worked on developing an efficient and accurate beam element for the finite element analysis of beams. There are a few studies about developing a nonlinear finite beam element in the literature. Researches are still continuing to develop several simpler and accurate elements that could lead an efficient solution for these types of problems.

Less number of nodes is a feature of a simple element. Increasing the number of nodes per element results in a larger global stiffness matrix of the problem. An important problem for beam element nonlinear problems is the shear locking. Full integration of shear strain energy enforces the constraints of kinematics interpolations, and the constraint dependents enforcement's on the rotational degree of freedom causes the normal rotations to be zero or constant. Then, bending energy vanishes. To sum up; the solution is 'locked' due to shear constraining and using shear correction factor shear locking might be avoided.

The literature survey given and reviewing of past and current studies and the goal of this study are in Chapter II.

The derivation of the element stiffness matrix starting from the virtual work principle is presented in Chapter III. The finite element solution method and algorithm of the code is explained at the end of the chapter.

In Chapter 4 the results obtained from the finite element analyses and discussions are included for the current work. Conclusion of the thesis and proposals for the future works are given in Chapter 5. The written code algorithm and flowchart are given in Appendix A.

CHAPTER II

LITERATURE SURVEY

2.1 Previous Studies

Bernoulli and Euler proposed a beam theory in the early 19th century which is later on named as 'Euler-Bernoulli Beam Theory' [1]. Their studies were not limited to small deflections but later Navier (1785-1836) consolidated the small displacement beam theory. Although linear analysis was accurate and adequate for many applications, for the nonlinear structures under ultimate limit states more realistic models have to be used. Especially developments in aerospace, offshore and construction applications have showed that simple, reliable and accurate non-linear formulations should have to be developed to model nonlinear analysis.

Geometric non-linear analysis has been pursued with three kinematic formulations which are total Lagrangian, updated Lagrangian and co-rotational. In the total Lagrangian the initial configuration is taken as the reference configuration where for the updated Lagrangian the configuration at last convergence is taken as the reference frame. In the co-rotational formulation a unique frame rotates with the element and it permits the use of linear kinematic relations, while the non-linear geometric behavior is accounted for the frame rotation.

The first non-linear geometric stiffness matrices were used in the early sixties [2, 3, 4]. But the real significant progress came after the incremental form for the updated Lagrangian and total Lagrangian formulations was developed [5]. After the incremental Lagrangian formulation is applied successively very effectively, it became very popular and applied to many other structures like thin-walled beam elements besides classical beams [6].

Timoshenko published the beam model that now bears his name, 'Timoshenko Beam Theory'. This was an extension of classical Euler-Bernoulli beam model. In his first studies Timoshenko introduced first order shear effects by releasing 'plane sections remain plane' which is a constraint for Euler-Bernoulli beam model. Not only that he also included rotational inertia in the kinetic energy [7].

Timoshenko beam theory was extended to include finite plane rotations and displacements in [8]. A three -dimensional finite beam element with large rotations was developed in [9, 10]. In those studies Lagrangian approach with small number of load increments based on rotation and displacement vector interpolations was used. The geometric stiffness matrix is non symmetric except at the equilibrium configuration under conservative load. A. Cardona and M. Geradin [11] presented a symmetric stiffness matrix with a different rotation discretization. Large rotations were first used with co-rotational formulation in [12]. The tangent matrix was not symmetric but the matrix could be artificially symmetrized to reduce the rate of convergence.

L.A. Crivelli and C.A. Felippa [13, 14] presented a nonlinear Timoshenko beam element with a limitation of hyper elastic and isotropic materials. By parametrizing the finite rotations suitably a symmetric geometric stiffness matrix is reached. A two node interpolation formulation is used.

M. Schulz and F. C. Filippou presented a spatial Timoshenko beam element with Lagrangian formulation [15]. The element is based on curvature interpolation that is independent of the rigid body motion of the beam element which simplifies the formulation. Generalized second order stress resultants are identified and the section response takes into account non-linear material behavior. Green-Lagrange strains are expressed in terms of section curvature and shear distortion. The first and second variations are functions of node displacements and rotations. A symmetric tangent stiffness matrix is derived by linearization and an iterative acceleration method is used for numerical convergence of hyper elastic materials. They also compared the numerical results of their study with the analytical results. The results of the numerical outputs and the analytical solution were in good agreement.

Z. Friedman and J.B Kosmatka [16] developed the stiffness, mass and consistent force matrices for a simple two-node Timoshenko beam element based upon Hamilton's principle. Cubic and quadratic Lagrangian polynomials are used for the transverse and rotational displacements, respectively, where the polynomials are made interdependent by requiring them to satisfy the two homogeneous differential equations associated with Timoshenko's beam theory. The resulting stiffness matrix, which can be exactly integrated and is free of 'shear-locking', is in

agreement with the exact Timoshenko beam stiffness matrix. Numerical results of their study showed that element exactly predicts the displacement of a short beam subjected to complex distributed loadings using only one element, and the element predicts shear and moment resultants and natural frequencies better than existing beam elements.

M. Eisenberger [17] studied derivation of shape functions for an exact 4-degree of freedom (dof) Timoshenko beam element. The difficulty was that of arriving at a superconvergent element with 4-dof, as is the case for the Bernuli-Euler classical beam element. Two different approaches are presented for the derivation of the shape functions. The first is based on the flexibility matrix, where utilizing the unit load method, including the term that accounts for the shear deformations in the virtual work expression, the stiffness matrix is derived. Then, a second method is presented to derive the exact shape functions, directly from the differential equations of the Timoshenko beam theory. The resulting shape functions are the same in both methods.

Seok-Soon Lee, Jeong-Seo Koo, Jin-Min Choi [18] presented a variational formulation for a Timoshenko beam element which is derived by the separation of the deformation mode into the bending deflection and shear deflection. Shear deflection is projected into bending deflection and the projection matrix is constructed by using the equilibrium equation and the relation of force and displacement. The exact stiffness matrix of the Timoshenko beam element can be obtained using their formulation. Examples and comparisons of their element with other elements are also given in their study.

J. M Wang [19] presented a study on the Timoshenko beam theory as an extension of the Euler-Bernoulli beam theory. The deflection and stress resultants of single-span Timoshenko beams, with general loading and boundary conditions, in terms of the corresponding Euler-Bernoulli beam solutions are derived in this study. The exact relationships developed allow engineering designers to readily obtain the bending solutions of Timoshenko beams from the familiar Euler-Bernoulli solutions without having to perform the more complicated flexural–shear-deformation analysis.

E. Yamaguchi, W.Kanok-Nukulchai, M. Hammadeh and Y. Kubo [20] proposed a finite-element formulation for the large displacement analysis of beams. It is based on the degeneration approach: The governing equations for a general solid are directly discretized. The assumptions of the Timoshenko beam theory are implemented in the discretization process by devising beam elements and utilizing the penalty method. The formulation for 2D beam analysis is first presented and the 3D formulation follows. Characteristically, the proposed beam elements possess relative nodes and rotations are excluded from nodal variables. The formulation they proposed for 3D beam analysis is just a simple extension of the 2D case, which can be attributed mainly to the avoidance of rotations in nodal variables. In numerical examples, the approximate penalty number is investigated first by analyzing a cantilever beam, and it is found as 10^3 times Young's modulus. With this value, example problems are solved and agreement with the existing solutions is observed, confirming the validity of the present formulation.

G. M. Kulikov and S. V. Plotnikova [21] presented a family of two-node hybrid stress–strain curved beam elements with four displacement degrees of freedom per node for the finite deformation 2D Timoshenko beam theory, which can be readily generalized on the two-node curved beam elements with six displacement dof for the 3D beam theory. The developed formulation is based on the principally new non-linear strain–displacement relationships that are objective, i.e., invariant under arbitrarily large rigid-body motions. To avoid shear and membrane locking and have no spurious zero energy modes, the assumed stress resultant and strain fields are invoked. In order to circumvent thickness locking, the modified material stiffness matrices corresponding to the plane stress state are employed. The fundamental unknowns consist of four displacements and five strains of the face lines of the beam, and five stress resultants. The element characteristic arrays are obtained by using the Hu-Washizu variational principle. To demonstrate the efficiency and accuracy of the formulation and to compare its performance with other non-linear finite element models reported in the literature, extensive numerical studies are presented in their study.

H. Antes [22] derived an integral equation description for all relevant states, the deflection, the rotation, the bending moment, and the shear forces. Adding the well known integral equations for axial displacements and forces in bars under tension, arbitrary plane frame structures is modelled by adequate combinations of these equations. Examples given demonstrate the applicability of this formulation as a first step to dynamic analyses of Timoshenko beam systems.

Moshe Eisenberger [23] derived the exact stiffness coefficients for a high order isotropic beam element. The terms are found directly from the solutions of the differential equations that describe the deformations of the cross-section according to the high order theory, which include cubic variation of the axial displacements over the cross-section of the beam. The model has six degrees of freedom at the two ends, one transverse displacement and two rotations, and the end forces are a shear force and two end moments. The equivalent end forces and moments for several cases of loading along the member are also given. The components of the end moments are investigated and a comparison is made with the Bernoulli–Euler and Timoshenko beam models.

Meeking and Rice [24] developed an Eulerian finite element formulation for problems of large elastic-plastic flow. The method was based on Hill's variational principle for incremental deformations. It could also be applied to isotropically hardening Prandtl-Reuss materials. The formulation could also be used for any conventional finite element program of small strain elastic plastic analysis, to be simply adapted to the problems of arbitrary amounts of deformation and arbitrary levels of stress in comparison to plastic deformation. The developed formulation was used with triangular three node element and the results obtained were quite reasonable.

Gotoh [25] proposed a formulation for large deformation and large strain analysis with material nonlinearity.

Nagtegaal, Parks and Rice [26] contributed to the literature a new variational principle which could be embedded into the existing finite

element codes which includes accurate computations to be made for even non suitable element designs. Numerical results obtained from a pure bending of a beam, a thick walled tube under pressure and deep double edge cracked tensile specimen showed that their formulation improved the previous results which were failing in some cases.

Baclund and Wennerström [27] presented a finite element analysis of arbitrary shape elastic-plastic analysis. The material was assumed to be isotropic and following the Von Misses yield criterion and Prandtl-Reuss flow rule. They obtained good results compared to the theoretical knowledge.

Argyris and Kleiber [28] presented numerical solution techniques of problems in continuum mechanics for the cases where there were finite elastic and plastic strain components with large deformations of configuration during loading process. Some approximations and some comparisons of natural approach and an intermediate reference configuration were made. This theory presented was applied with triangular elements and calculated elastic strains were found quite different than results from purely Eulerian formulation. Some refinements to this theory were presented by Argyris, Doltsinis and Kleiber [29].

Argyris and Doltsinis [30] developed a formulation in quasistatic and isothermal deformation process and non isothermal and dynamic problems. Their study was extension of large strain elastic processes natural approach which has been started by [31] and then developed by [32, 33]. In the first part of the study stress-strain relations were obtained

using total elastic and incremental plastic deformations. For the solution a new algorithm developed for unifying the Newton technique with respect to geometric nonlinearity and the iteration process with respect to the material nonlinearity. The results of the numerical examples presented in this study were satisfactory since their results were still deviating in the plastic zone when compared to the exact or experimental results.

Chandre and Mukherjee [34] presented a finite element formulation for elasto-viscoplastic problems in case of large strains and deformations. The computer program developed performed quite satisfactory results but the computation time should be decreased.

Lu and Yee [35] presented how to succeed on direct and accurate evaluation of singular integrals in the sense of Cauchy principal values and weakly singular integrals over quadratic boundary elements in the three dimensional stress analysis and internal cells in two dimensional elastic-plastic analyses. A quadratic polar coordinate transformation technique was applied to reduce the singularity order of integrals and then Stoke's theorem was used to remove the singularity in the Cauchy principle value integrals. The evaluation of these integrals could be performed by standard Gauss quadrature. Numerical examples performed with triangular and rectangular elements of two dimensional and three dimensional elastic plastic problems showed the effectiveness of the method.

Axelsson and Samuelsson [36] introduced the derivation of constitutive equations which display isotropic and kinematic hardening characteristics

for the elastic-plastic two dimensional structures. The program developed has the option to select an optimal combination of iteration procedures.

Simo [37] presented a technique based on the principle of maximum plastic dissipation. The implementation of the hyperelastic J_2 -flow theory was shown to decrease to a trivial modification of classical radial return algorithm which is agreeable to linearization. Objective rates and incrementally objective algorithms played no role in the approach. The rates of convergence of the iterative solution procedure should be insensitive to mesh size.

Simo, Kennedy and Taylor [38] developed a formulation on the principle of maximum plastic dissipation which was exploited to construct mixed finite element for elasto-plasticity.

Rajiyah, Okada and Atluri [39] developed a boundary integral equation for velocity gradients in a finite strain elastic-plastic solid. When the integral equations are differentiated to derive a relation for velocity gradients some singularities are observed. But the method they derived do not involve these singularities. They applied their theory to a thick cylinder and the results they obtained were pretty good when compared to other classical methods.

Moran, Shih and Ortiz [40] proposed an approach which includes decomposition of the deformation gradients into two separate parts: elastic and plastic terms. They also discussed some computational and constitutive aspects of finite deformation plasticity.

For the time integration of elastic-plastic constitutive equations Gratacos, Montmitonnet and Chenot [41] derived a generalized midpoint rule. The optimal choice of the parameter of midpoint rule could be computed by referencing to the analytical solution assuming no work hardening.

Ristinmaa and Tryding [42] presented an approach which established exact integration of constitutive equations in elasto-plasticity. In this approach total strain was assumed to be constant. This approach also included some closed-form solutions which were derived for combined kinematics and isotropic hardening. For Von Mises' materials kinematic and isotropic hardening characteristics and Mohr-Coulomb and Tresca materials they worked on specifically.

Osias and Swedlow [43] developed an application which was using Galerkin method to linear differential equations of quasi-linear model. They established the numerical solution capabilities for plane strain and stress problems.

Bathe and Özdemir [44] presented two consistent formulations for elastic-plastic large deformation analysis in which one of the initial or current configurations is used for determining static and kinematic variables. By the two different formulations quite accurate and identical results could be obtained. The formulations were experimented with the large deformation analyses of beams and shells and the results were reasonable when compared to the exact solutions.

Caddemi and Mardin [45] presented a continuous, time discrete formulation of the loading of an elastic, perfectly plastic body governed by von Misses yield criteria. The Newton-Raphson scheme was used to have an iterative solution of the nonlinear programming problem. If an elastic modulus were used in this problem the scheme converges smoothly. But if a tangent predictor was used a line search algorithm should be included to make convergence real.

Borst and Mühlhaus [46] proposed a plasticity theory which states yield strength depending not only on equivalent plastic strain measure but also on the Laplacian. For appropriate boundaries starting from variational method the same formulation could also be derived.

Miehe [47] discussed multiplicative elasto-plasticity for large plastic and large elastic strains.

Shu and Tai-Hua [48] developed an approach named equivalent force method for destructive structural analyses of elastic-plastic problems. They also compared the numerical results with the former finite element results to demonstrate the precision of the present method.

2.2 Present Study

In this study an efficient beam element for large deformation of materially nonlinear problems is developed. The finite element method used in this thesis has several advantages, such as easily imposing boundary conditions and no prior assumptions are to be made on deformations. In this thesis all nonlinear terms are included. Elastic-plastic analysis is applied to solve large deformation beam problems with different loading and boundary conditions [49, 50].

The body motion is expressed by using Updated Lagrangian Approach which has been preferred to model large deformation problem [51].

CHAPTER III

FORMULATION and GOVERNING EQUATIONS

In this chapter, the derivation of element stiffness matrix and stress strain relations is presented by using the procedure given in [50, 51]. The virtual work principle and the updated Lagrangian formulation are used. Material is assumed to be isotropic and rate sensitive obeying J_2 flow rule. Work hardening characteristics of material is considered and all nonlinear terms are included. A two node iso-parametric beam element is used. A layered structure is used to model through-the-thickness distribution of elastic and plastic zones.

And finite element program developed will be introduced as well.

3.1 Virtual Work Principle

For the undeformed and deformed configurations of a body shown in Figure 3.1, \mathbf{N} and \mathbf{n} are the unit normal vectors of the areas dS^0 and dS , \mathbf{X} and \mathbf{x} are the coordinates of a material point at the undeformed and deformed states, respectively. The first Piola – Kirchoff stress tensor $\tilde{\mathbf{T}}$ gives the actual force $d\mathbf{P}$ on the deformed infinitesimal area, dS , but it is reckoned per unit area of the undeformed infinitesimal area, dS^0 .

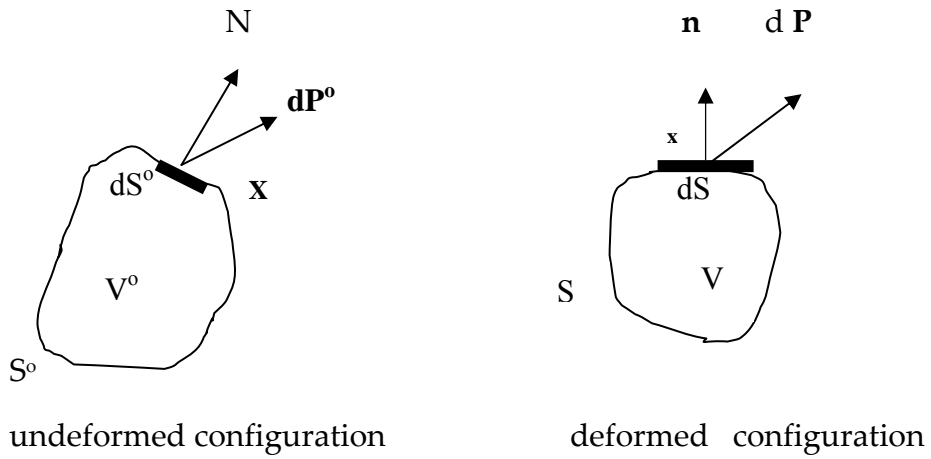


Figure 3.1 An infinitesimal body in the deformed and undeformed configurations.

It can be written that [52]

$$\mathbf{T}dS^0 = \mathbf{t} dS \tag{3.1}$$

where \mathbf{T} is the surface traction in the undeformed state and \mathbf{t} is the state surface traction in the deformed state.

Also

$$\mathbf{T} = \mathbf{N} \cdot \tilde{\mathbf{T}} \tag{3.2}$$

where $\tilde{\mathbf{T}}$ is the first Piola-Kirchoff stress tensor.

The relation between the first Piola-Kirchoff stress tensor and the second Piola-Kirchoff stress tensor, $\tilde{\mathbf{S}}$, is given as

$$\tilde{\mathbf{T}} = \tilde{\mathbf{S}} \cdot \tilde{\mathbf{F}}^T \quad 3.3$$

where $\tilde{\mathbf{F}}$ is the deformation gradient tensor. For a virtual displacement $\delta \mathbf{x}$ the external virtual work, neglecting the body forces, is stated as

$$\delta W_{\text{ext}} = \int_S \mathbf{t} \cdot \delta \mathbf{x} dS \quad 3.4$$

for the deformed configuration by using Equations 3.1 and 3.2 the above equation becomes

$$\delta W_{\text{ext}} = \int_S \mathbf{T} \cdot \delta \mathbf{x} dS^0 = \int_{S^0} \mathbf{N} \cdot \tilde{\mathbf{T}} \cdot \delta \mathbf{x} dS^0 \quad 3.5$$

Transforming the surface integral over S^0 to a volume integral V^0 Equation 3.5 can be expressed as

$$\delta W_{\text{ext}} = \int_{V^0} \tilde{\mathbf{T}} : \delta \tilde{\mathbf{F}}^T dV^0 \quad 3.6$$

then

$$\int_{V^0} \tilde{\mathbf{T}} : \delta \tilde{\mathbf{F}} dV^0 = \int_{S^0} \mathbf{T} \cdot \delta \mathbf{x} dS^0 \quad 3.7$$

Writing the above Equation 3.7 for the second Piola-Kirchoff stress tensor by using Equation 3.3 [52, 53];

$$\int_{V^0} \tilde{\mathbf{S}} : \delta \tilde{\mathbf{E}} dV^0 = \int_{S^0} \mathbf{T} \cdot \delta \mathbf{x} dS^0 \quad 3.8$$

where \mathbf{E} is the Lagrangian strain tensor. Writing it in Cartesian coordinate system in indicial notation

$$\int_{V^0} S_{ij} \delta E_{ij} dV^0 = \int_{S^0} T_k \delta x_k dS^0 \quad 3.9$$

Taking the material time derivative of the above equation gives

$$\int_{V^0} (\dot{S}_{ij} \delta E_{ij} + S_{ij} \delta \dot{E}_{ij}) dV^0 = \int_{S^0} \dot{T}_k \delta x_k dS^0 \quad 3.10$$

where

$$E_{ij} = \frac{1}{2} \left[\frac{\partial x_k}{\partial X_i} \frac{\partial x_k}{\partial X_j} - \delta_{ij} \right] \quad 3.11$$

and

$$\delta E_{ij} = \frac{1}{2} \left[\delta \frac{\partial x_k}{\partial X_i} \frac{\partial x_k}{\partial X_j} + \frac{\partial x_k}{\partial X_i} \delta \frac{\partial x_k}{\partial X_j} \right] \quad 3.12$$

or

$$\delta E_{ij} = \frac{1}{2} \left[\frac{\delta \partial x_k}{\partial X_i} \frac{\partial x_k}{\partial X_j} + \frac{\partial x_k}{\partial X_i} \frac{\delta \partial x_k}{\partial X_j} \right] \quad 3.13$$

The above equation can also be written as

$$\delta E_{ij} = \frac{1}{2} \left[\frac{\partial \delta x_k}{\partial x_1} \frac{\partial x_1}{\partial X_i} \frac{\partial x_k}{\partial X_j} + \frac{\partial x_k}{\partial X_i} \frac{\partial \delta x_k}{\partial x_1} \frac{\partial x_1}{\partial X_j} \right] \quad 3.14$$

The material derivative of the virtual change of Lagrangian strain tensor can be written as

$$\delta \dot{E}_{ij} = \frac{1}{2} \left[\frac{\delta \partial x_k}{\partial X_i} \frac{\partial v_k}{\partial x_1} \frac{\partial x_1}{\partial X_j} + \frac{\partial v_k}{\partial x_1} \frac{\partial x_1}{\partial X_i} \frac{\delta \partial x_k}{\partial X_j} \right] \quad 3.15a$$

or the above equation can also be written as

$$\delta \dot{E}_{ij} = \frac{1}{2} \left[\frac{\delta \partial x_k}{\partial x_m} \frac{\partial x_m}{\partial X_i} \frac{\partial v_k}{\partial x_1} \frac{\partial x_1}{\partial X_j} + \frac{\partial v_k}{\partial x_1} \frac{\partial x_1}{\partial X_i} \frac{\delta \partial x_k}{\partial x_m} \frac{\partial x_m}{\partial X_j} \right] \quad 3.15b$$

The second Piola-Kirchoff stress tensor can be written as [52, 53]

$$S_{ij} = j \frac{\partial X_i}{\partial x_k} \sigma_{kl} \frac{\partial X_j}{\partial x_l} \quad 3.16$$

where j is the deformation gradient tensor determinant and σ is the Cauchy stress tensor. Using

$$\frac{D}{Dt} \left(\frac{\partial X_i}{\partial x_k} \right) = \frac{\partial v_m}{\partial x_k} \frac{\partial X_i}{\partial x_m} \quad 3.17$$

and

$$\frac{Dj}{Dt} = j \frac{\partial v_m}{\partial x_m} \quad 3.18$$

then taking the material time derivative of Equation 3.18

$$\begin{aligned} \dot{S}_{ij} &= j \frac{\partial v_m}{\partial x_m} \frac{\partial X_i}{\partial x_k} \sigma_{kl} \frac{\partial X_j}{\partial x_1} - j \frac{\partial v_k}{\partial x_m} \frac{\partial X_i}{\partial x_k} \sigma_{ml} \frac{\partial X_j}{\partial x_1} + j \frac{\partial X_i}{\partial x_k} \dot{\sigma}_{kl} \frac{\partial X_j}{\partial x_1} - j \frac{\partial X_i}{\partial x_k} \sigma_{km} \frac{\partial v_l}{\partial x_m} \frac{\partial X_j}{\partial x_1} \\ &= j \frac{\partial X_i}{\partial x_k} \left[\frac{\partial v_m}{\partial x_m} \sigma_{kl} - \frac{\partial v_k}{\partial x_m} \sigma_{ml} + \dot{\sigma}_{kl} - \sigma_{km} \frac{\partial v_l}{\partial x_m} \right] \frac{\partial X_j}{\partial x_1} \end{aligned} \quad 3.19$$

where $\left[\frac{\partial v_m}{\partial x_m} \sigma_{kl} - \frac{\partial v_k}{\partial x_m} \sigma_{ml} + \dot{\sigma}_{kl} - \sigma_{km} \frac{\partial v_l}{\partial x_m} \right]$ is the Truesdell stress rate tensor, $\bar{\sigma}_{kl}$ [52].

Then the material time derivative can also be written as

$$\dot{S}_{ij} = j \frac{\partial X_i}{\partial x_k} \bar{\sigma}_{kl} \frac{\partial X_j}{\partial x_1} \quad 3.20$$

Turning back to Equation 3.10 ; the left hand side term can be obtained by using Equation 3.14 and Equation 3.20 as

$$\begin{aligned}
\dot{S}_{ij}\delta E_{ij} &= \frac{1}{2}j\frac{\partial X_i}{\partial x_p}\bar{\sigma}_{pq}\frac{\partial X_j}{\partial x_q}\frac{\partial \delta x_k}{\partial x_1}\frac{\partial x_l}{\partial X_i}\frac{\partial x_k}{\partial X_j} + \frac{1}{2}j\frac{\partial X_i}{\partial x_p}\bar{\sigma}_{pq}\frac{\partial X_j}{\partial x_q}\frac{\partial x_k}{\partial X_i}\frac{\partial \delta x_k}{\partial x_1}\frac{\partial x_l}{\partial X_j} \\
&= \frac{1}{2}j\delta_{lp}\delta_{kq}\bar{\sigma}_{pq}\frac{\partial \delta x_k}{\partial x_1} + \frac{1}{2}j\delta_{kp}\delta_{lq}\bar{\sigma}_{pq}\frac{\partial \delta x_k}{\partial x_1} \\
&= \frac{1}{2}j\bar{\sigma}_{lk}\frac{\partial \delta x_k}{\partial x_1} + \frac{1}{2}j\bar{\sigma}_{kl}\frac{\partial \delta x_k}{\partial x_1}
\end{aligned} \tag{3.21}$$

Finally one gets

$$\dot{S}_{ij}\delta E_{ij} = j\bar{\sigma}_{kl}\frac{\partial \delta x_k}{\partial x_1} \tag{3.22}$$

And the second term of Equation 3.10 is obtained from Equation 3.15 and Equation 3.18

$$\begin{aligned}
S_{ij}\delta \dot{E}_{ij} &= \frac{1}{2}j\frac{\partial X_i}{\partial x_p}\sigma_{pq}\frac{\partial X_j}{\partial x_q}\frac{\partial \delta x_k}{\partial x_m}\frac{\partial x_m}{\partial X_i}\frac{\partial v_k}{\partial x_1}\frac{\partial x_l}{\partial X_j} \\
&+ \frac{1}{2}j\frac{\partial X_i}{\partial x_p}\sigma_{pq}\frac{\partial X_j}{\partial x_q}\frac{\partial v_k}{\partial x_1}\frac{\partial x_l}{\partial X_i}\frac{\partial \delta x_k}{\partial x_m}\frac{\partial x_m}{\partial X_j} \\
&= \frac{1}{2}j\left[\delta_{mp}\delta_{lq}\sigma_{pq}\frac{\partial v_k}{\partial x_1}\frac{\partial \delta x_k}{\partial x_m} + \delta_{lp}\delta_{mq}\sigma_{pq}\frac{\partial v_k}{\partial x_1}\frac{\partial \delta x_k}{\partial x_m}\right] \\
&= \frac{1}{2}j[\sigma_{ml} + \sigma_{lm}]\frac{\partial v_k}{\partial x_1}\frac{\partial \delta x_k}{\partial x_m}
\end{aligned} \tag{3.23}$$

finally one can end up with

$$S_{ij}\delta\dot{E}_{ij} = j\sigma_{ml}\frac{\partial v_k}{\partial x_l}\frac{\partial\delta x_k}{\partial x_m} \quad 3.24$$

Substituting Equation 3.22 and 3.24 into equation 3.10

$$\int_{V_0}\left(j\bar{\sigma}_{kl}\frac{\partial\delta x_k}{\partial x_l} + j\sigma_{ml}\frac{\partial v_k}{\partial x_l}\frac{\partial\delta x_k}{\partial x_m}\right)dV^0 = \int_{S_0}\dot{T}_k\delta x_k dS^0 \quad 3.25$$

dividing Equation 3.25 by δt , virtual time one can write the above equation in a new form [50]

$$\int_{V_0}\left(j\left(\bar{\sigma}_{kl}\frac{\partial\delta v_k}{\partial x_l} + \sigma_{ml}\frac{\partial v_k}{\partial x_l}\frac{\partial\delta v_k}{\partial x_m}\right)\right)dV^0 = \int_{S_0}\dot{T}_k\delta v_k dS^0 \quad 3.26$$

The velocity gradient can be written in two separate terms one is for the deformations where the other is for the rotations. Then

$$\frac{\partial v_k}{\partial x_l} = D_{kl} + W_{kl} \quad 3.27$$

D_{kl} is the rate of deformation tensor which is symmetric and W_{kl} is the spin tensor which is unsymmetric part of the Equation 3.27. The definition of the deformation tensor and the spin tensor is given as

$$D_{mn} = \frac{1}{2} \left[\frac{\partial v_m}{\partial x_n} + \frac{\partial v_n}{\partial x_m} \right] \quad 3.28a$$

$$W_{mn} = \frac{1}{2} \left[\frac{\partial v_m}{\partial x_n} - \frac{\partial v_n}{\partial x_m} \right] \quad 3.28b$$

Thus

$$\frac{\partial \delta v_k}{\partial x_l} = \delta D_{kl} + \delta W_{kl} \quad 3.29$$

Rewriting Equation 3.26

$$\int_{V_0} j \left(\bar{\sigma}_{kl} (\delta D_{kl} + \delta W_{kl}) + \sigma_{ml} \frac{\partial v_k}{\partial x_l} \frac{\partial \delta v_k}{\partial x_m} \right) dV^0 = \int_{S_0} \dot{T}_k \delta v_k dS^0 \quad 3.30$$

or

$$\int_{V_0} j \left(\bar{\sigma}_{kl} \delta D_{kl} + \sigma_{ml} \frac{\partial v_k}{\partial x_l} \frac{\partial \delta v_k}{\partial x_m} \right) dV^0 = \int_{S_0} \dot{T}_k \delta v_k dS^0 \quad 3.31$$

observing that Truesdell stress rate tensor can be written as [49, 50, 52]

$$\bar{\sigma}_{kl} = \sigma_{kl}^* + \frac{\partial v_m}{\partial x_m} \sigma_{kl} - \sigma_{km} D_{lm} - \sigma_{ml} D_{km} \quad 3.32$$

σ_{kl}^* is the Jaumann rate of Cauchy stress tensor.

So, Equation 3.31 can be written as

$$\int_{V_0} \mathbf{j} \left[\left(\sigma_{kl}^* \delta D_{kl} + \frac{\partial v_m}{\partial x_m} \sigma_{kl} \delta D_{kl} - \sigma_{km} D_{lm} \delta D_{kl} - \sigma_{ml} D_{km} \delta D_{kl} \right) + \sigma_{ml} \frac{\partial v_k}{\partial x_l} \frac{\partial \delta v_k}{\partial x_m} \right] dV^0$$

3.33

$$= \int_{S_0} \mathbf{T}_k \delta v_k dS^0$$

and finally Equation 3.34 is obtained as

$$\int_{V_0} \mathbf{j} \left[\left(\sigma_{kl}^* + \frac{\partial v_m}{\partial x_m} \sigma_{kl} \right) \delta D_{kl} - 2\sigma_{ml} D_{km} \delta D_{kl} + \sigma_{ml} \frac{\partial v_k}{\partial x_l} \frac{\partial \delta v_k}{\partial x_m} \right] dV^0$$

3.34

$$= \int_{S_n} \mathbf{T}_k \delta v_k dS^0$$

Since in the Updated Lagrangian method all variables are referred to the configuration at time t and the displacements, strains and stresses corresponding to time $t+\Delta t$ are wanted to be solved, it can be written that

$$\tilde{\mathbf{F}} = \tilde{\mathbf{F}}^{-1} \approx \tilde{\mathbf{I}}$$

3.35

and also

$$\det(\mathbf{F}) \approx 1$$

3.36

In this case Cauchy and Kirchoff stress tensors are identical for an incompressible material ($j \approx 1$)

$$\sigma_{ij} = \tau_{ij}$$

3.37

where by definition

$$\tau_{ij} = j\sigma_{ij} \quad 3.38$$

and their stress rates are related through [50]

$$\tau_{kl}^* = \sigma_{kl}^* + \frac{\partial v_m}{\partial x_m} \sigma_{kl} \quad 3.39$$

Then one can get the following equation

$$\begin{aligned} & \int_{V_o} j \left[(\tau_{kl}^* \delta D_{kl} - 2\sigma_{ml} D_{km} \delta D_{kl} + \sigma_{ml} \frac{\partial v_k}{\partial x_l} \frac{\partial \delta v_k}{\partial x_m}) \right] dV_o \\ & = \int_{S_n} \dot{T}_k \delta v_k dS_o \end{aligned} \quad 3.40$$

The constitutive elastic-plastic equation in the rate form can be expressed as follows

$$\dot{\sigma}_{kl} = C_{klmn} D_{mn} \quad 3.41$$

where $\dot{\sigma}_{kl}$ is not objective. The above constitutive equation can also be expressed in terms of Jaumann stress rate as follows

$$\sigma_{kl}^* = C_{klmn} D_{mn} \quad 3.42$$

where σ_{kl}^* is objective. From the Equation 3.39

$$\tau_{kl}^* = j\sigma_{kl}^* + j\dot{\sigma}_{kl} \quad 3.43$$

and since $j \approx 1$ and $j \ll 1$

One can rewrite Equation 3.42 as

$$\tau_{kl}^* = C_{klmn} D_{mn} \quad 3.44$$

Then equation 3.40 becomes

$$\int_{V_0} \left[C_{klmn} D_{mn} \delta D_{kl} - 2\sigma_{ml} D_{km} \delta D_{kl} + \sigma_{ml} \frac{\partial v_k}{\partial x_l} \frac{\partial \delta v_k}{\partial x_m} \right] dv \quad 3.45$$

$$= \int_S \dot{T}_k \delta v_k dS$$

Equation 3.45 can be rewritten in matrix form as

$$\int_V (\delta D^T C D - 2\delta D^T \sigma_1 D + \delta W^T \sigma_2 W) dv = \int_{S_n} \dot{T}_k \delta v^T dS \quad 3.46$$

where the matrices σ_1 and σ_2 are appropriately formed matrices.

3.2 Virtual Work Formulation of Nodal Variables

3.2.1 Displacement Field of the Timoshenko Beam

The velocity field of a beam element whose mid-surface coincides with x-y plane can be expressed as;

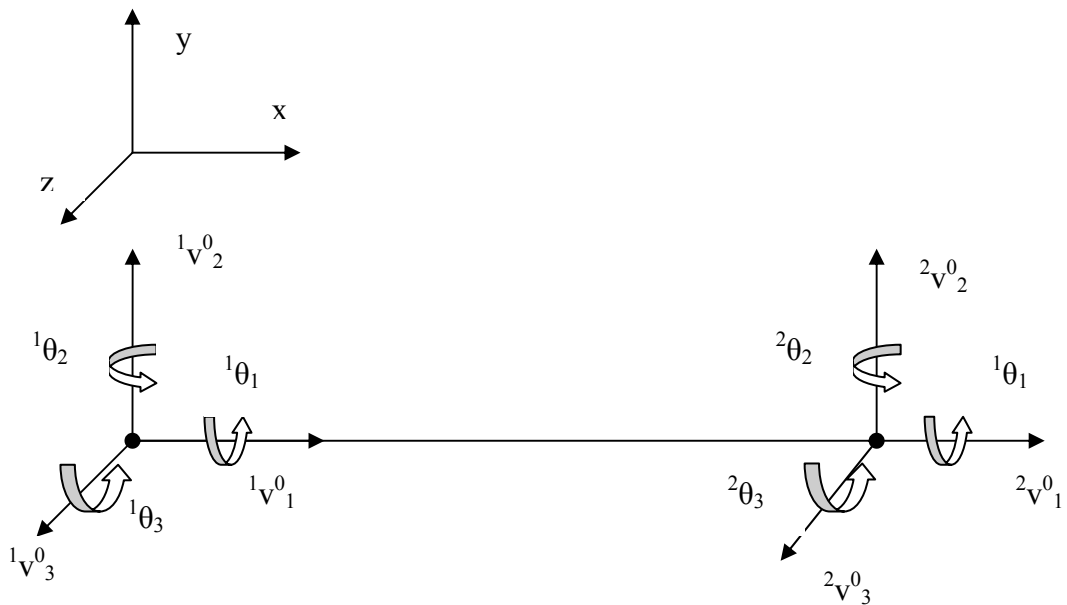


Fig 3.2 3D Beam Element Nodal Variables

$$\begin{aligned}
 u_1(x_1, t) &= u_1^o(x_1, t) + x_3\theta_2(x_1, t) - x_2\theta_3(x_1, t) \\
 u_2(x_1, t) &= u_2^o(x_1, t) - x_3\theta_1(x_1, t) \\
 u_3(x_1, t) &= u_3^o(x_1, t) + x_2\theta_1(x_1, t)
 \end{aligned}
 \tag{3.47}$$

3.2.2 Two Dimensional Beam Element

In this section a two dimensional beam element formulation will be developed for elastic-plastic analysis. The beam has three nodal variables at each node (Fig 3.3). These are the axial displacements denoted as u_1 in the $+x$ direction, v_1 in the $+y$ direction and the rotation θ_3 in the $+z$ direction.

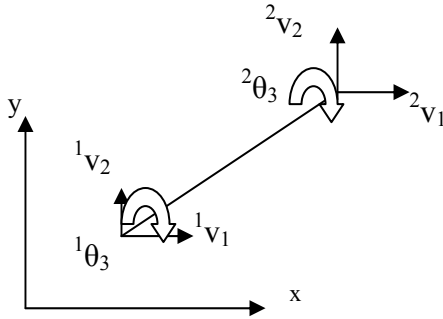


Fig 3.3 Two Dimensional Beam Element Nodal Variables

The displacement field can be written as

$$\begin{aligned} u_1(x_1, x_2, t) &= u_1^0(x_1, t) - x_2 \theta_3(x_1, t) \\ u_2(x_1, x_2, t) &= u_2^0(x_1, t) \end{aligned} \quad 3.48$$

The velocity field of a beam element whose mid-surface coincides with x - y plane can be expressed as

$$\begin{aligned} v_1(x_1, x_2, t) &= v_1^0(x_1, t) - x_2 \beta_3(x_1, t) \\ v_2(x_1, x_2, t) &= v_2^0(x_1, t) \end{aligned} \quad 3.49$$

where v_1 and v_2 are the velocities and β_3 is time rate of the rotation θ_3 .

In order to prevent shear locking iso-parametric Timoshenko beam element with linear kinematic interpolations will be used. The iso-parametric beam element as seen in Fig 3.4 is chosen to simplify the problem and get an efficient way to be used for the evaluation of derivatives and integrals while forming the stiffness and equivalent nodal loads since by this approach one can use the coordinates that are consonant with the local geometry.

The displacements and rotations are

$$\begin{aligned} v_1 &= L_1^{-1} v_1^0 + L_2^{-2} v_1^0 \\ v_2 &= L_1^{-1} v_2^0 + L_2^{-2} v_2^0 \\ \beta_3 &= L_1^{-1} \beta_3 + L_2^{-2} \beta_3 \end{aligned} \tag{3.50}$$

where $L=L_1 + L_2$ and

$$L_1 = L(1 - x/L) \tag{3.51a}$$

$$L_2 = L(x/L) \tag{3.51b}$$

as shown in Fig 3.4. The location of any third point can be written by dimensionless length coordinates

$$\xi_1 = \frac{L_1}{L} \quad \text{and} \quad \xi_2 = \frac{L_2}{L} \tag{3.52}$$

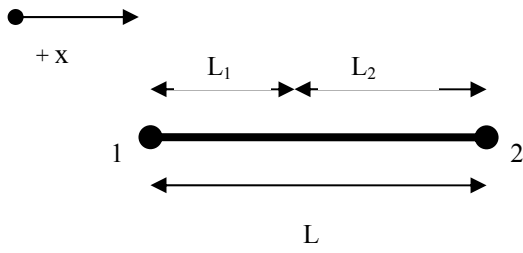


Fig 3.4 The iso-parametric beam element

and

$\xi_1 + \xi_2 = 1$ which shows that ξ_1 and ξ_2 are dependent on each other.

Now it is possible to express the global coordinate x in terms of local coordinates ξ_1 and ξ_2 .

Thus

$$x = \xi_1 x_1 + \xi_2 x_2 \quad 3.53$$

The rate of deformation matrix can be written explicitly as

$$D_{11} = \frac{1}{2} \left(\frac{\partial v_1}{\partial x_1} + \frac{\partial v_1}{\partial x_1} \right) = \frac{\partial v_1}{\partial x_1} = \frac{\partial v_1^0}{\partial x_1} - x_2 \frac{\partial \beta_3}{\partial x_1} \quad 3.54a$$

$$D_{11} = v_{1,1}^0 - x_2 \beta_{3,1}$$

$$D_{12} = \frac{1}{2} \left(\frac{\partial v_1}{\partial x_2} + \frac{\partial v_2}{\partial x_1} \right) = \frac{1}{2} (-\beta_3 + \frac{\partial v_2^0}{\partial x_1}) \quad 3.54b$$

$$D_{12} = \frac{1}{2} (v_{2,1}^0 - \beta_3)$$

Equations 3.54a and 3.54b can be written in matrix form as $D=HD^*$

$$\begin{bmatrix} D_{11} \\ 2D_{12} \end{bmatrix} = \begin{bmatrix} 1 & -x_2 & 0 \\ 0 & 0 & 1 \end{bmatrix} \begin{bmatrix} v_{1,1}^0 \\ \beta_{3,1} \\ v_{2,1}^0 - \beta_3 \end{bmatrix} \quad 3.55a$$

where

$$H = \begin{bmatrix} 1 & -x_2 & 0 \\ 0 & 0 & 1 \end{bmatrix} \quad 3.55b$$

and

$$D^* = \begin{bmatrix} v_{1,1}^0 \\ \beta_{3,1} \\ v_{2,1}^0 - \beta_3 \end{bmatrix} \quad 3.55c$$

Hence $D = HD^*$ The matrix D^* can be written as

$$D^* = B^* q \quad 3.55d$$

In the above equation q is the nodal variable vector determined as

$$q = \begin{bmatrix} {}^1v_1^0 \\ {}^1v_2^0 \\ {}^1\beta_3 \\ {}^1v_1^0 \\ {}^1v_2^0 \\ {}^1\beta_3 \end{bmatrix} \quad 3.56a$$

and B^* matrix is

$$B^* = \begin{bmatrix} L_{1,x} & 0 & 0 & L_{2,x} & 0 & 0 \\ 0 & 0 & L_{1,x} & 0 & 0 & L_{2,x} \\ 0 & L_{1,x} & -L_1 & 0 & L_{2,x} & -L_{2,x} \end{bmatrix} \quad 3.56b$$

The derivatives of the nodal velocities with respect to coordinates are

$$v_{1,1} = \frac{\partial v_1}{\partial x_1} = \frac{\partial v_1^0}{\partial x_1} - x_2 \frac{\partial \beta_3}{\partial x_1} = v_{1,1}^0 - x_2 \beta_{3,1} \quad 3.57a$$

$$v_{1,2} = \frac{\partial v_1}{\partial x_2} = -\beta_3 \quad 3.57b$$

$$v_{2,1} = \frac{\partial v_2}{\partial x_1} = v_{2,1}^0 \quad 3.57c$$

$$v_{2,2} = \frac{\partial v_2}{\partial x_2} = 0 \quad 3.57d$$

Taking the derivative of the velocities and the rotation using the shape functions

$$\begin{aligned} v_{1,1} &= L_{1,1}^1 v_1^0 + L_{2,1}^2 v_1^0 \\ v_{2,1} &= L_{1,1}^1 v_2^0 + L_{2,1}^2 v_2^0 \\ \beta_{3,1} &= L_{1,1}^1 \beta_3 + L_{2,1}^2 \beta_3 \end{aligned} \quad 3.58$$

From the above equations the spin tensor can be formed as

$$W = \begin{bmatrix} v_{1,1} \\ v_{1,2} \\ v_{2,1} \end{bmatrix} = \begin{bmatrix} v_{1,1}^0 - x_2 \beta_{3,1} \\ -\beta_3 \\ v_{2,1}^0 \end{bmatrix} \quad 3.59a$$

or $W = GW^*$ as

$$W = \begin{bmatrix} v_{1,1} \\ v_{1,2} \\ v_{2,1} \end{bmatrix} = \begin{bmatrix} 1 & 0 & 0 & -x_2 \\ 0 & 0 & -1 & 0 \\ 0 & 1 & 0 & 0 \end{bmatrix} \begin{bmatrix} v_{1,1}^0 \\ v_{2,1}^0 \\ \beta_3 \\ \beta_{3,1} \end{bmatrix} \quad 3.59b$$

where

$$G = \begin{bmatrix} 1 & 0 & 0 & -x_2 \\ 0 & 0 & -1 & 0 \\ 0 & 1 & 0 & 0 \end{bmatrix} \quad 3.59c$$

and

$$W^* = \begin{bmatrix} v_{1,1} \\ v_{2,1} \\ \beta_3 \\ \beta_{3,1} \end{bmatrix} \quad 3.59d$$

Defining

$$W^* = M^* q \quad 3.60$$

M^* matrix is formed as

$$M^* = \begin{bmatrix} L_{1,x} & 0 & 0 & L_{2,x} & 0 & 0 \\ 0 & L_{1,x} & 0 & 0 & L_{2,x} & 0 \\ 0 & 0 & L_1 & 0 & 0 & L_2 \\ 0 & 0 & L_{1,x} & 0 & 0 & L_{2,x} \end{bmatrix} \quad 3.61$$

The stress field can be written as

$$\begin{bmatrix} \sigma_{11} \\ \sigma_{12} \end{bmatrix} = \begin{bmatrix} C_{11} & C_{12} \\ C_{21} & C_{22} \end{bmatrix} \begin{bmatrix} D_{11} \\ D_{12} \end{bmatrix} \quad 3.62$$

or

$$\sigma = CD \quad 3.63$$

Turning back one can write the first term of Equation 3.46 as

$$\begin{aligned} \int_V D^T C D dv &= \int_V D^{*T} H^T C H D^* dV \\ &= \int_S \int_{h_n}^{h_{n+1}} D^{*T} H^T C H D^* dz dS \\ &= \int_S D^{*T} C^* D^* dS \end{aligned} \quad 3.64a$$

where

$$C^* = \int_{h_n}^{h_{n+1}} H^T C H dz \quad 3.64b$$

where “n” is the layer number . So finally Equation 3.64a becomes

$$\begin{aligned} \int_S D^{*T} C^* D^* dv &= \int_V \delta \dot{q}^T B^{*T} C^* B^* \dot{q}^* dS \\ &= \delta \dot{q}^{*T} \left[\int_S B^{*T} C^* B^* dS \right] \dot{q} \end{aligned} \quad 3.65$$

The second term in Equation 3.46 can be written as

$$\begin{aligned}
\int_S 2\delta D^T \sigma_1 D dv &= \int_V 2D^{*T} H^T \sigma_1 H D^* dv \\
&= \int_S \int_{h_n}^{h_{n+1}} 2D^{*T} H^T \sigma_1 H D^* dz dS \\
&= \int_S 2D^{*T} \sigma^* D^* dS
\end{aligned} \tag{3.66}$$

where

$$\sigma_1^* = \int_{h_n}^{h_{n+1}} H^T \sigma_1 H dz \tag{3.67}$$

Rewriting it as

$$\begin{aligned}
\int_V 2\delta D^T \sigma_1 D dV &= \int_S \delta \dot{q}^{*T} B^{*T} \sigma_1^* B^* \dot{q}^* dS \\
&= \delta \dot{q}^{*T} \left[\int_S B^{*T} \sigma_1^* B^* dS \right] \dot{q}
\end{aligned} \tag{3.68}$$

and the last term in the Equation 3.46 can be written as

$$\begin{aligned}
\int_S W^T \sigma_2 W dv &= \int_V W^{*T} G^{*T} \sigma_2 G W^* dv \\
&= \int_S W^{*T} \sigma_2^* W^* dS
\end{aligned} \tag{3.69}$$

where

$$\sigma_2^* = \int_{h_n}^{h_{n+1}} G^T \sigma_1 G dz \tag{3.70}$$

finally Equation 3.71 is obtained as

$$\begin{aligned} \int_V \delta W^T \sigma_2 W dv &= \int_S \delta \dot{q}^{*T} M^{*T} \sigma_2^* M^* \dot{q}^* dS \\ &= \delta \dot{q}^{*T} \left[\int_S M^{*T} \sigma_2^* M^* dS \right] \dot{q} \end{aligned} \quad 3.71$$

Then the equation Equation 3.46 becomes

$$\begin{aligned} \delta \dot{q}^{*T} \left[\int_S B^{*T} C^* B^* dS \right] \dot{q}^* - \delta \dot{q}^{*T} \left[\int_S 2B^{*T} \sigma_1^* B^* dS \right] \dot{q}^* \\ + \delta \dot{q}^{*T} \left[\int_S M^{*T} \sigma_2^* M^* dS \right] \dot{q} = \int_S \delta \dot{q}^{*T} N^{*T} \dot{T} dS \end{aligned} \quad 3.72$$

Eliminating $\delta \dot{q}^{*T}$ from the above Equation 3.72 we end up with

$$\left[\int_S \left(B^{*T} C^* B^* - 2B^{*T} \sigma_1^* B^* + M^{*T} \sigma_2^* M^* \right) dS \right] \dot{q}^* = \int_S N^{*T} \dot{T} dS \quad 3.73$$

3.3 Constitutive Relation

The stress-strain relationship is given by a well known equation called Prandtl-Reuss equations [54] which can be written as separately

$$D_{ij} = \frac{1+\gamma}{E} \dot{\sigma}_{ij} - \frac{\gamma}{E} \delta_{ij} \dot{\sigma}_{kk} \quad 3.74$$

for elastic loading and unloading the above Equation 3.74 becomes

$$D_{ij} = \frac{1+\gamma}{E} \dot{\sigma}_{ij} - \frac{\gamma}{E} \delta_{ij} \dot{\sigma}_{kk} + \frac{9\sigma'_{ij} \sigma'_{kl} \dot{\sigma}'_{kl}}{4h\bar{\sigma}^2} \quad 3.75$$

for plastic loading where

γ : Poisson's Ratio

E : Young's Modulus

$$\sigma' = \text{Deviatoric Stress} = \sigma_{ij} - \frac{1}{3} \delta_{ij} \sigma_{kk}$$

$$\bar{\sigma} = \text{Equivalent Stress} = \sqrt{\frac{3}{2} (\sigma'_{ij} \sigma'_{ij})}$$

h : Slope of Cauchy stress-logarithmic plastic strain curve for a simple tension test

δ : Kronecker Delta

Finally

$$D_{ij} = \left[\frac{1+\gamma}{E} \delta_{ik} \delta_{jl} - \frac{\gamma}{E} \delta_{ij} \delta_{kl} + \frac{9\sigma'_{ij} \sigma'_{kl}}{4h\bar{\sigma}^2} \right] \dot{\sigma}_{kl} \quad 3.76$$

where

$k=0$ for elastic loading

$k=1$ for plastic loading

or in matrix form

$$D=C^{-1} \sigma \quad 3.77$$

3.4 Global Stiffness Matrix

The global stiffness matrix is obtained by assembling the element stiffness matrices. After obtaining the displacements the stresses and strains can be easily determined from these displacements.

The relation between rate of external force applied and the nodal velocities are given as

$$K_i V_i = \Delta \dot{F}_i^{\text{ext}} \quad 3.78$$

where

K_i : the element stiffness matrix

V_i : the nodal velocity vector

\dot{F}_i^{ext} : rate of external force vector of the i^{th} element

when the Equation 3.73 is considered

$$K_i = \left[\int_S \left(B^{*\text{T}} C^* B^* - 2B^{*\text{T}} \sigma^* B^* + M^{*\text{T}} \sigma^* M^* \right) dS \right] \quad 3.79$$

$$V_i = \dot{q}^* \quad 3.80$$

$$\dot{F}_i^{\text{ext}} = \int_S N^{*\text{T}} \dot{T} dS \quad 3.81$$

Then the structure stiffness matrix can be written as

$$K = \sum K_i \quad 3.82$$

Then the global stiffness matrix becomes

$$KV_i = \dot{F}^{\text{ext}} \quad 3.83$$

3.5 The Newton-Raphson Method

Most popular method used to solve for such kind of nonlinear problems is the Newton-Raphson method. It is an iterative solution scheme and has some modified solution methods as well for different kind of problems in order to obtain more realistic and exact results. In this thesis Newton-Raphson iteration scheme is used as well and implemented to the code [51].

The incremental finite element equation that governs the response of the finite element system in an arbitrary load increment is

$$[K^{i-1}]^{\text{gl}} V^i = \dot{F}^{\text{ext}} - \dot{R}^{i-1} \quad 3.84$$

where $[K^{i-1}]^{\text{gl}}$ is the global stiffness matrix of the system V^i is the vector of nodal velocities.

\dot{F}^{ext} is the vector of rate of externally applied nodal point loads,

\dot{R}^{i-1} is the vector rate of nodal point forces corresponding to the internal

element stresses and the superscript i-1 is used to denote the i-1'st approximation. The resulting change in nodal velocities is

$$\mathbf{V}^i = \left[\left[\mathbf{K} \right]_{\text{gl}}^{i-1} \right]^{-1} \mathbf{f}^{\text{ext}} \quad 3.85$$

The change in rate of nodal force $\Delta \dot{\mathbf{R}}_{\text{el}}^i$ which is in equilibrium with the stress change calculated for element n may be found as

$$\dot{\mathbf{R}}_{\text{el}}^i = \int_{\mathbf{V}} \mathbf{B}^{*T} \mathbf{H}^T \dot{\boldsymbol{\sigma}}^i d\mathbf{V} \quad 3.86$$

or it can be rewritten as

$$\dot{\mathbf{R}}_{\text{el}}^i = \int_{\mathbf{V}} \mathbf{B}^{*T} \left[\int_{h_n}^{h_{n+1}} [\mathbf{H}]^T \dot{\boldsymbol{\sigma}}^i dz \right] d\mathbf{A} \quad 3.87$$

here iteration is carried out over the volume of the nth element. Summing up all the equilibrium force changes for all adjoining elements permit us forming the global array $\Delta \dot{\mathbf{R}}^i$ which is also in equilibrium with the calculated change in stress throughout the mesh.

Generally because of the nonlinearity of stiffness relationships, this rate of force vector will never be the same as the applied external load. A correction to the stiffness matrix can be evaluated by updating the stiffness matrix at every iteration as required in Newton-Raphson procedure.

Thus

$${}^{t+\Delta t} [V^i]^{i+1} = \left[\left[{}^{t+\Delta t} [K^i]^{gl} \right]^{-1} \right] {}^{t+\Delta t} [f^{ext}]^{i+1} \quad 3.88$$

The iteration procedure is repeated until the convergence criteria determined will be reached. The nodal displacement for an increment is the sum of the displacement changes calculated for all the iteration within that increment.

3. 6 Convergence Criteria

Iteration method is used to solve for incremental problems in which a criteria for terminating the iteration is defined. If the results of successive iterations are within the previously defined range then the iteration is terminated and next time increment is applied.

After determination of the convergence criteria another problem occurs due to the formulation fluctuations.

In this thesis the displacements obtained for every iteration from the nodal velocity vectors are compared with the previous iteration to ensure that they are within the convergence criteria.

The convergence can be written down as;

$$\frac{\|\Delta u^i\|}{\|{}^{t+\Delta t} \Delta u^i\|} \leq \text{CONVERGENCE CRITERIA}$$

$$\text{where } \|u\| = \left(\sum_{i=1}^n |u_i|^2 \right)^{0.5}$$

The convergence criteria predefined for each analysis and the iteration of the solution is continued up to iteration i until the condition given above is satisfied. The vector u at time $t+\Delta t$ should be approximated. The best solution for this to use the last value obtained as a previous approximation to get a better result.

To specify the convergence criteria can be a very tough job sometimes because of the nature of the problem. Defining the criteria accurately will directly affect the results of the finite element program. It also affects the computation time a lot in case of large number of elements and equations. Specifically for nonlinear beam element problem this criteria should be carefully defined because of the large deformation effects and the nature of the nonlinear problem which here is used in the Updated Lagrangian approach. This approach takes the initial values not the reference configuration but the lastly obtained configuration as the reference configuration. The value used in this thesis for convergence factor is 0.02 which in some cases may encounter problems to converge when force increment is changed.

3.7 The Solution Procedures

To develop an effective finite element program with minimum computation time skyline technique is used in this thesis [51].

A vector can be defined in which i^{th} element gives the equation number that corresponds to the element degree of freedom i . This array can be found from the nodal points to which the element is connected and the equation numbers that is assigned to the nodal points. The element stiffness matrix then can be assigned to the structure stiffness matrix by using the specific storage scheme [51].

Since the global stiffness matrix is symmetric and banded only the upper part of the matrix can be taken into account with the bandwidth. This means the number of elements to be stored in the array is reduced due to the above scheme taking only the elements below "skyline". This means zero elements are not taken into account above the "skyline " although they are in the bandwidth. This helps to reduce the stored elements which would lead to much less computing time and high efficiency. If one defines the row number of the first element which is not zero in column i as m_i the variables m_i $i=1, \dots, n$ define the skyline of the matrix where the variables $(i-m_i)$ are defining the column heights. The column height can be defined from the connectivity element arrays. Also the half-bandwidth of the stiffness matrix, m_k , equals maximum $\max (i-m_i)$. Since the column heights vary with i all zero elements above skyline should not be included into the solution procedure.

But the zero elements within the skyline of the matrix should be included into the solution procedure since they will probably end up with nonzero elements at the end due to the calculations. Once column heights of the matrix is defined the elements are stored in an array named, {A}. Then an array called MAXA(I) is also defined to store the addresses of the diagonal elements of the structure stiffness matrix in {A}. The addresses of the i^{th} diagonal element in the original stiffness matrix, K_{ii} in {A} is MAXA{I}, it is noted that MAXA(I) is equal to the sum of the column heights up to (i-1) is column plus 1. The number of nonzero elements in the i^{th} column of the original stiffness matrix is equal to MAXA(I+1)-MAXA(I) and the element addresses goes on like MAXA(I),MAXA(I)+1.....

By using the method described above all the nonzero elements existing can be addressed and used in further calculations by addressing them easily.

The above procedure is developed and published by Bathe [51]. Also in the previous works this procedure is successfully used for elastic plastic finite element code [49, 50].

3.8 Algorithm for the Finite Element Code

The code developed for this thesis is basically to develop several subroutines and functions and runs successively one after the other to print out the results. The code is tried to be written as much as flexible in order to make necessary changes during the thesis work and to be understandable and adaptable for future thesis works.

For this purpose here the algorithm of the code is given:

- i. Input data is taken from the initially prepared separate file which includes global coordinates of the nodes, material properties and constants, nodal degree of freedoms, element connectivity and forces applied externally to the nodes.
- ii. Increase the load which is previously divided into several load steps at the beginning
- iii. Build the necessary transformation matrices between the local and global coordinates, shape functions, local node coordinates and the effective beam element lengths
- iv. Calculate the elastic or elastic –plastic constitutive matrix
- v. Build the element stiffness matrix in a separate subroutine
- vi. Transfer element stiffness matrix from local coordinates to global coordinates
- vii. Build the global stiffness matrix
- viii. Construct the global force vector
- ix. Calculate the global displacements from the global equation solution.

- x. Calculate stresses and strains
- xi. Check whether the elements are within the elastic range or they are in the elastic-plastic region by comparing the stresses obtained in step x. with the yield point of the material. If the element is in the plastic region the constitutive equation belongs to plastic case are used for that element.
- xii. Check whether the convergence criteria reached or not. If the criteria is not reached turn back to step iii and repeat up to step xii.
- xiii. Check whether total load is reached. If it is not reached turn back to step ii and repeat the steps.
- xiv. Print out the final obtained data such as final coordinates of the nodes, stresses of the elements, strains of the elements and the layers of the elements.

The flowchart of the program is given in Appendix A .

CHAPTER IV

RESULTS AND DISCUSSION

A number of experiments have been conducted to compare the results with the numerical ones. In the experiments, a cantilever beam and a beam clamped from both ends have been considered.

The properties of the metal used were obtained by the simple tension test. The stress-strain relation of the material is given in Appendix B.

In order to obtain the experimental data, meshes are scribed on the specimens. After applying the load, the new position of mesh is measured to determine the deformation.

4.1 Case I : Specimen Clamped from One Side

In this section, results of the experiment and the finite element program are compared for a cantilever beam loaded by a force of 50 N at the free end. The length, width and the thickness of the beam are 280 mm, 25.2 mm and 2.68 mm, respectively.

In the finite element analyses 280 elements with 281 nodes have been used (Fig 4.1).

In the experiments deformations of the beam corresponding to 35 N, 40 N, 45N and 50 N loads are determined.

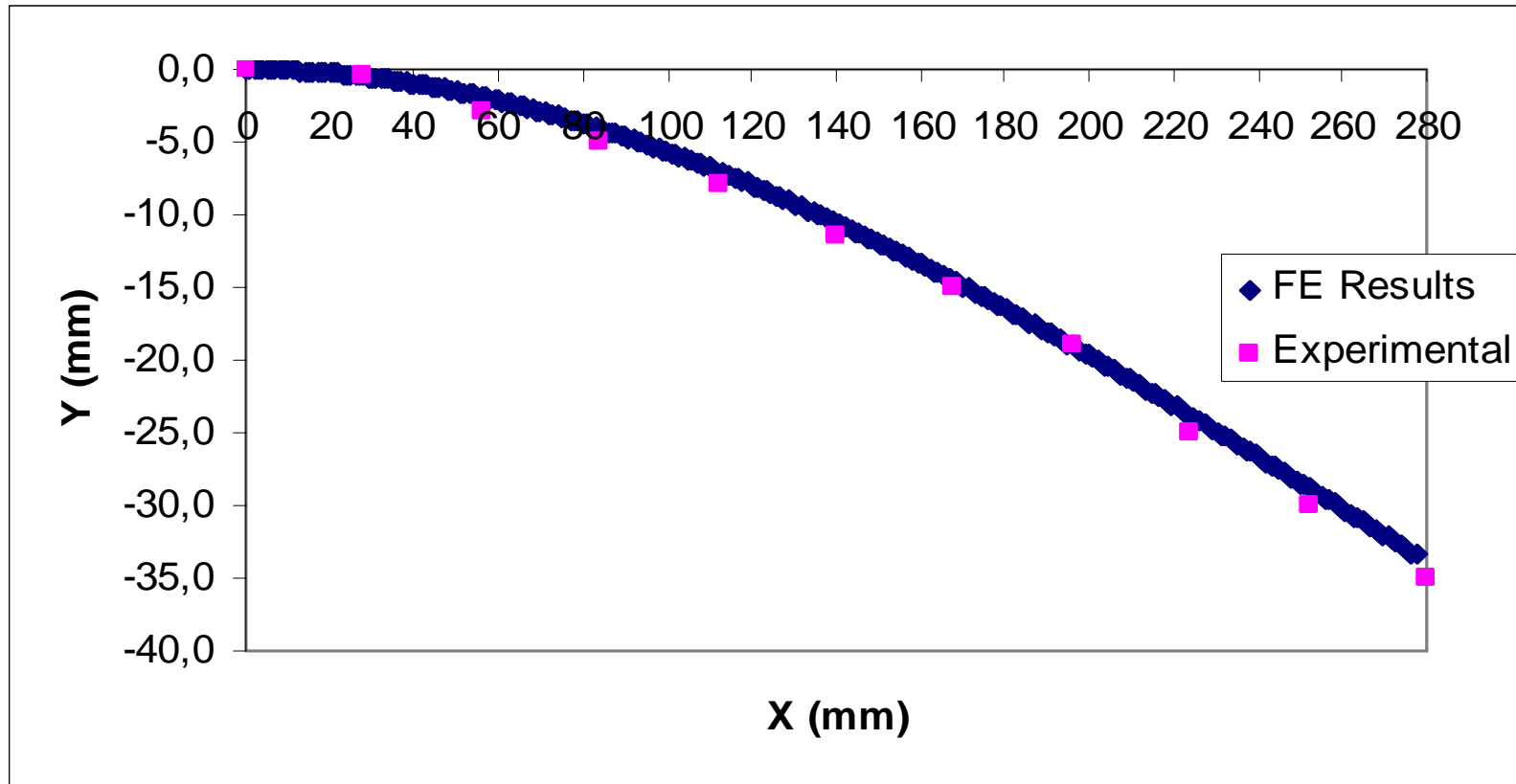
For this purpose the beam is fixed from one end, a force is applied from the free end by hanging the load and increasing the magnitude gradually. By drawing the mesh on the beam the displacements of the points from the horizontal is measured and compared with the numerical outputs.

The experimental and numerical results are given in Figure 4.2. Also the elements deformed plastically for different loading conditions are shown in Figure 4.3.

In Figure 4.3, each grid stands for 28 elements. The shaded zones show that majority of 28 elements in that zone are in the plastic range.



Fig 4.1 Loading and boundary conditions used for specimen clamped from one side.



(a)

Fig 4. 2 Deflections Obtained from Experiments and Finite Elements for a 2,68 mm Specimen Clamped from One Side Under the Loads a)35N, b)40 N, c)45 N, d)50 N

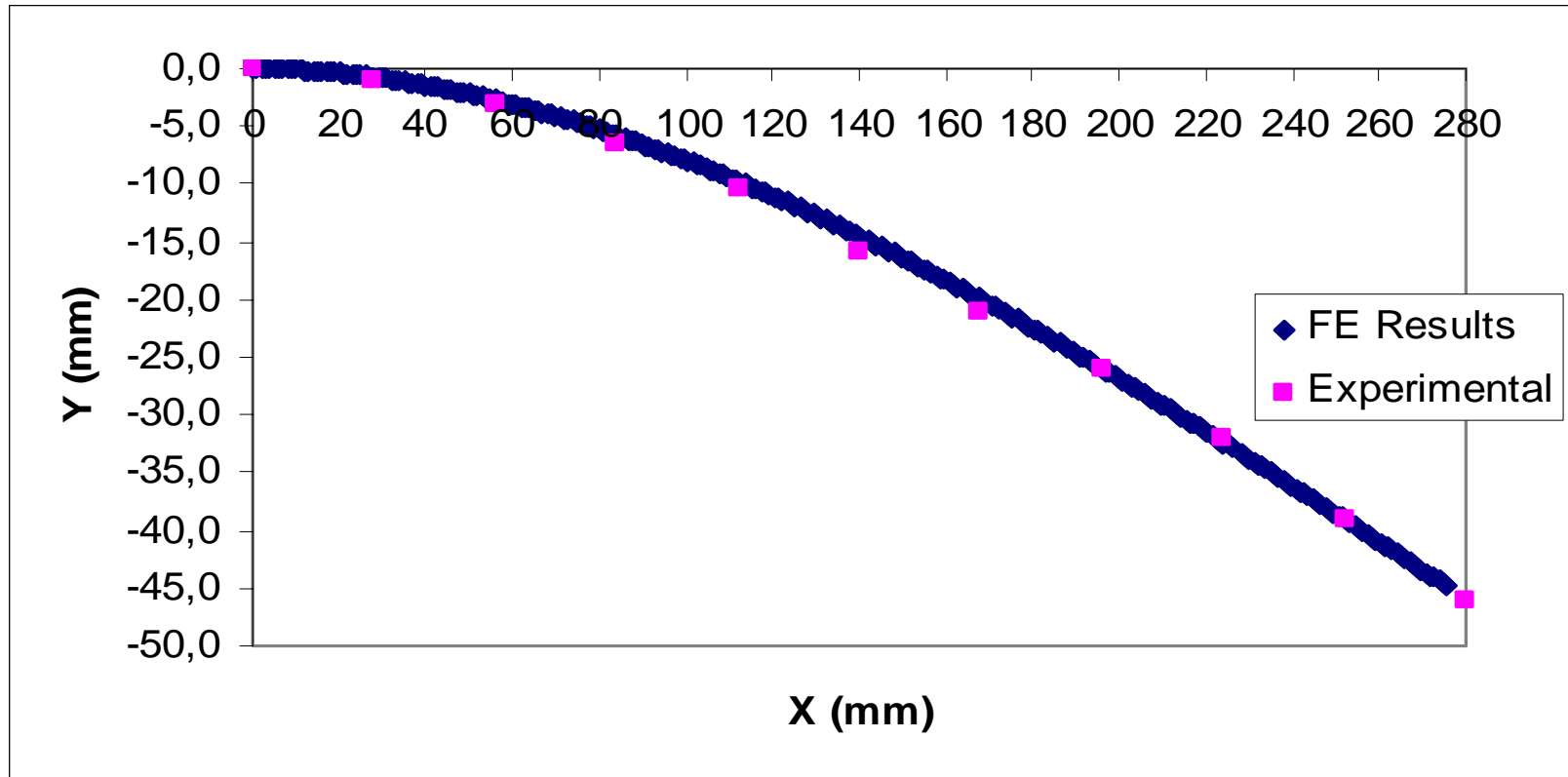


Fig 4. 2 (Continue)

(b)

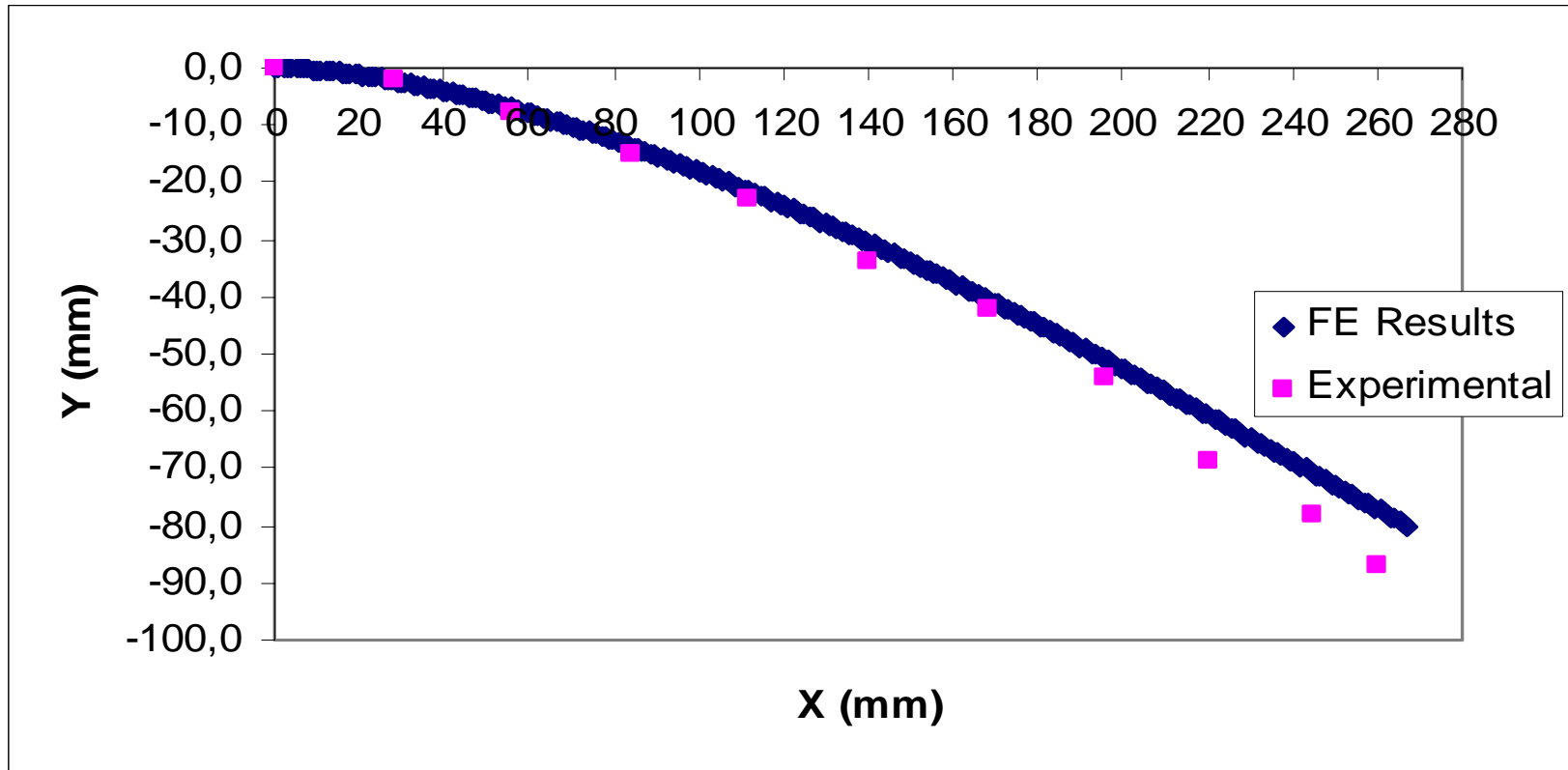


Fig 4.2 (Continue)

(c)

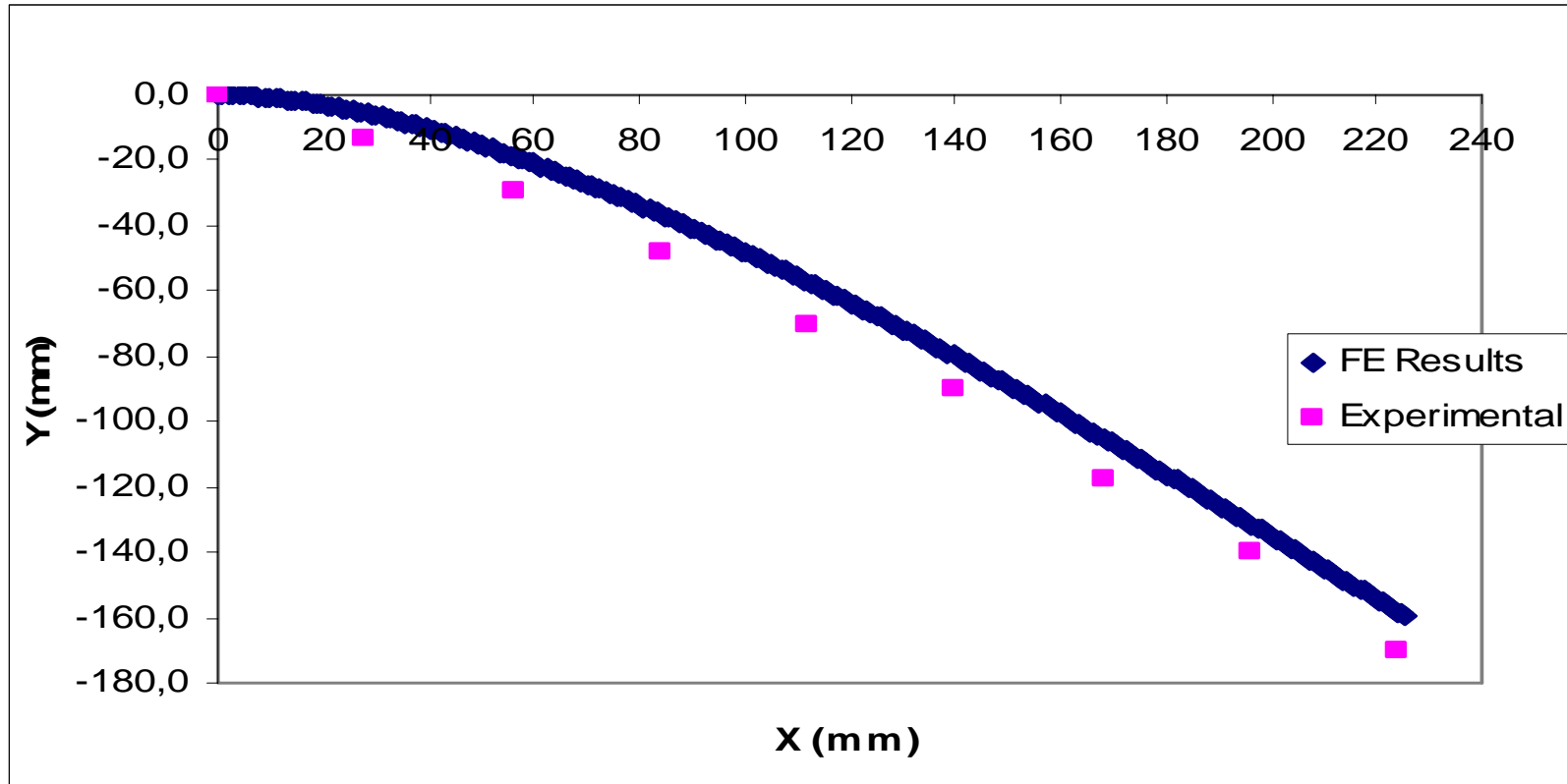
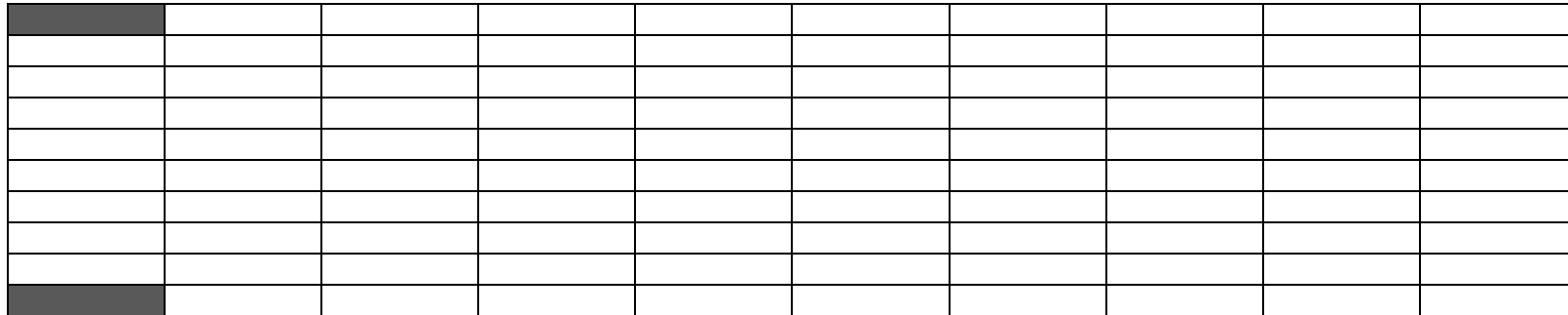
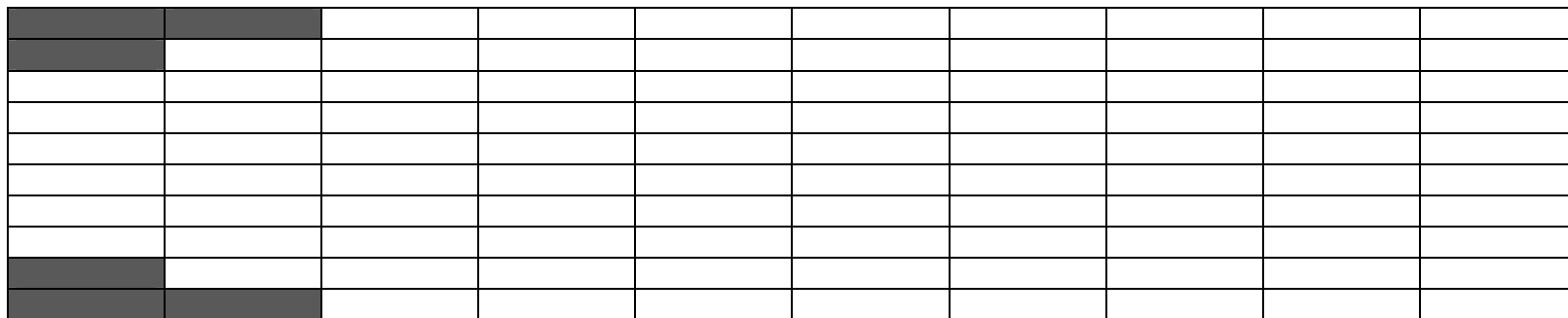


Fig 4.2 (Continue)

(d)



(a)



(b)

Fig. 4.3 Elements Deformed Plastically at a) 40 mm b) 50 mm c) 60 mm d) 70 mm e) 80 mm f) 90 mm g) 100 mm
h) 110mm i) 120 mm j) 130 mm k)140 mm l) 150 mm m) 160 mm n) 165 mm

(e)

(f)

Fig. 4.3 (Continue)

(g)

(h)

Fig. 4.3 (Continue)

4.2 Case II: Specimen Clamped from Two Sides

In this section, numerical results of the experiment and the finite element program are compared for the deformation of a two ends fixed beam. The length, width and the thickness of the beam is 280 mm, 25.2 mm and 2.68 mm, respectively.

In the finite element analyses 280 elements with 281 nodes have been used (Fig 4.4). The beam is fixed from both end, a force is applied from the mid-point by hanging the load and increasing the magnitude gradually. By drawing the mesh over the beam the displacements of the points from the horizontal is measured and compared.

In the experiments the force is applied gradually and deformations of the beam corresponding to 50 N, 100 N, 150 N and 200 N are determined. (Fig 4.5). Figure 4.6 gives the plastically deformed elements for different mid-point deflections. In Figure 4.6, every column stands for 28 elements. That means the shaded zones show that majority of 28 elements in that zone are in the plastic range.

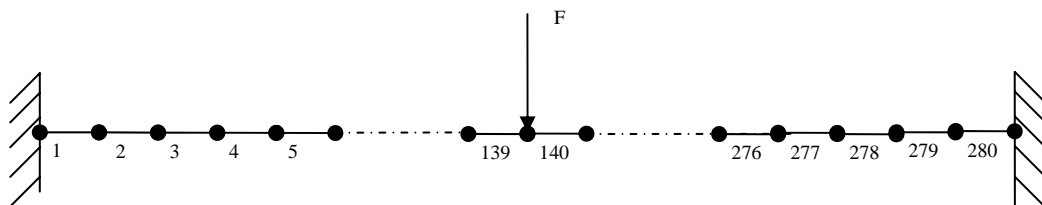
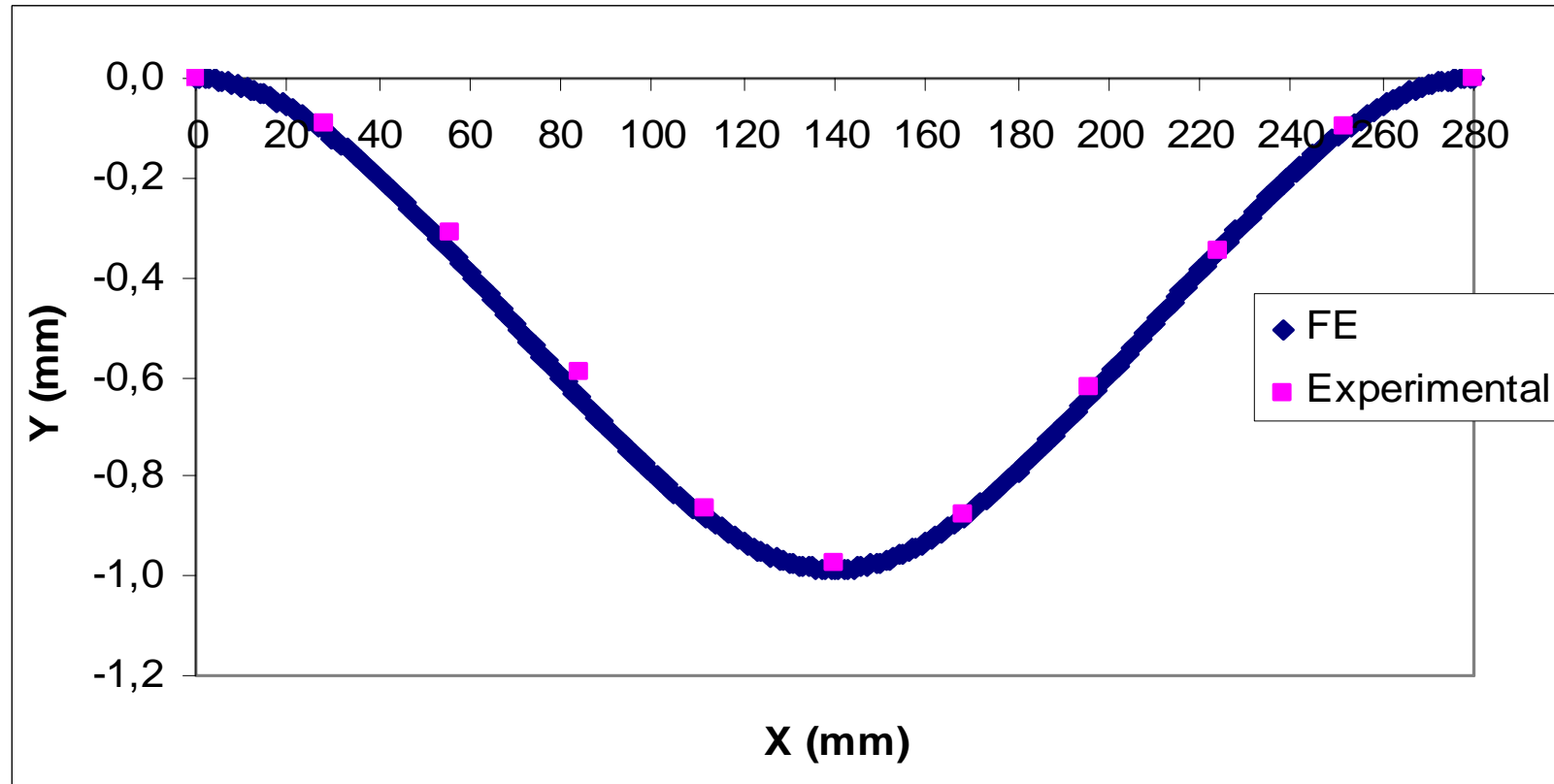


Fig 4.4 Loading and boundary conditions used for specimen clamped from two sides



(a)

Fig 4. 5 Deflections Obtained for a Test specimen Clamped from Two Sides Under the Loads a) 50N b)100 N
c)150 N d)200 N

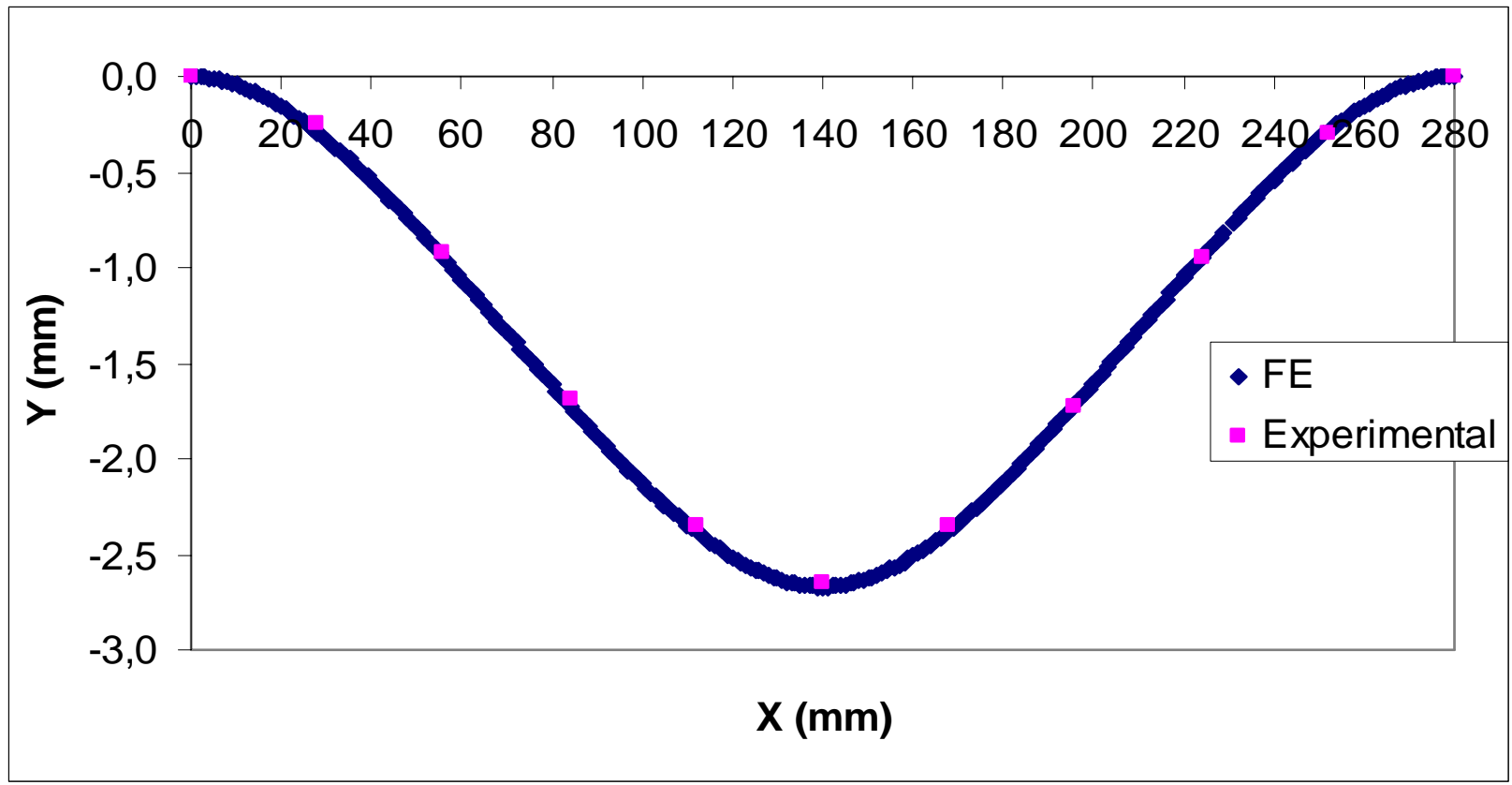


Fig 4.5 (Continue)

(b)

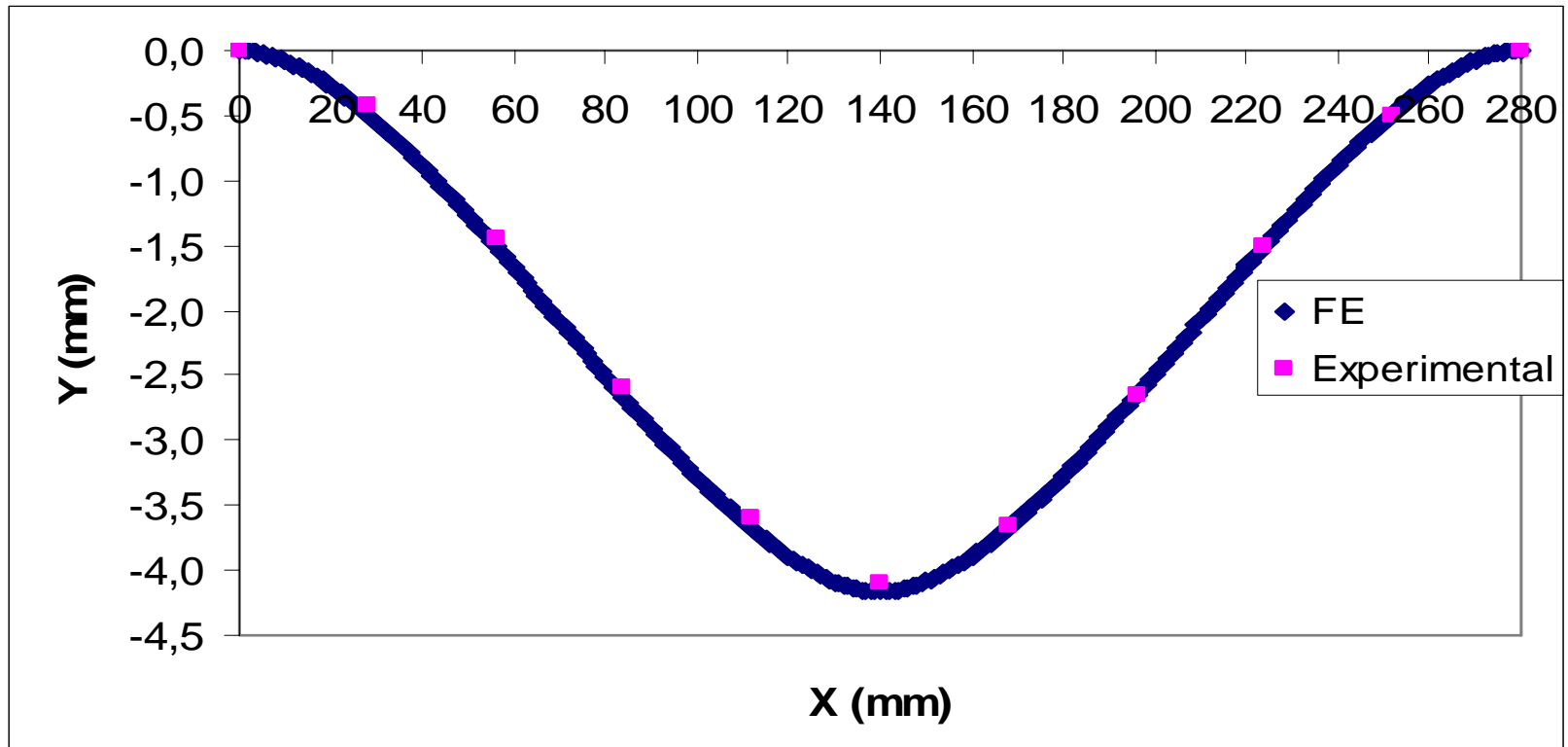


Fig 4.5 (Continue)

(c)

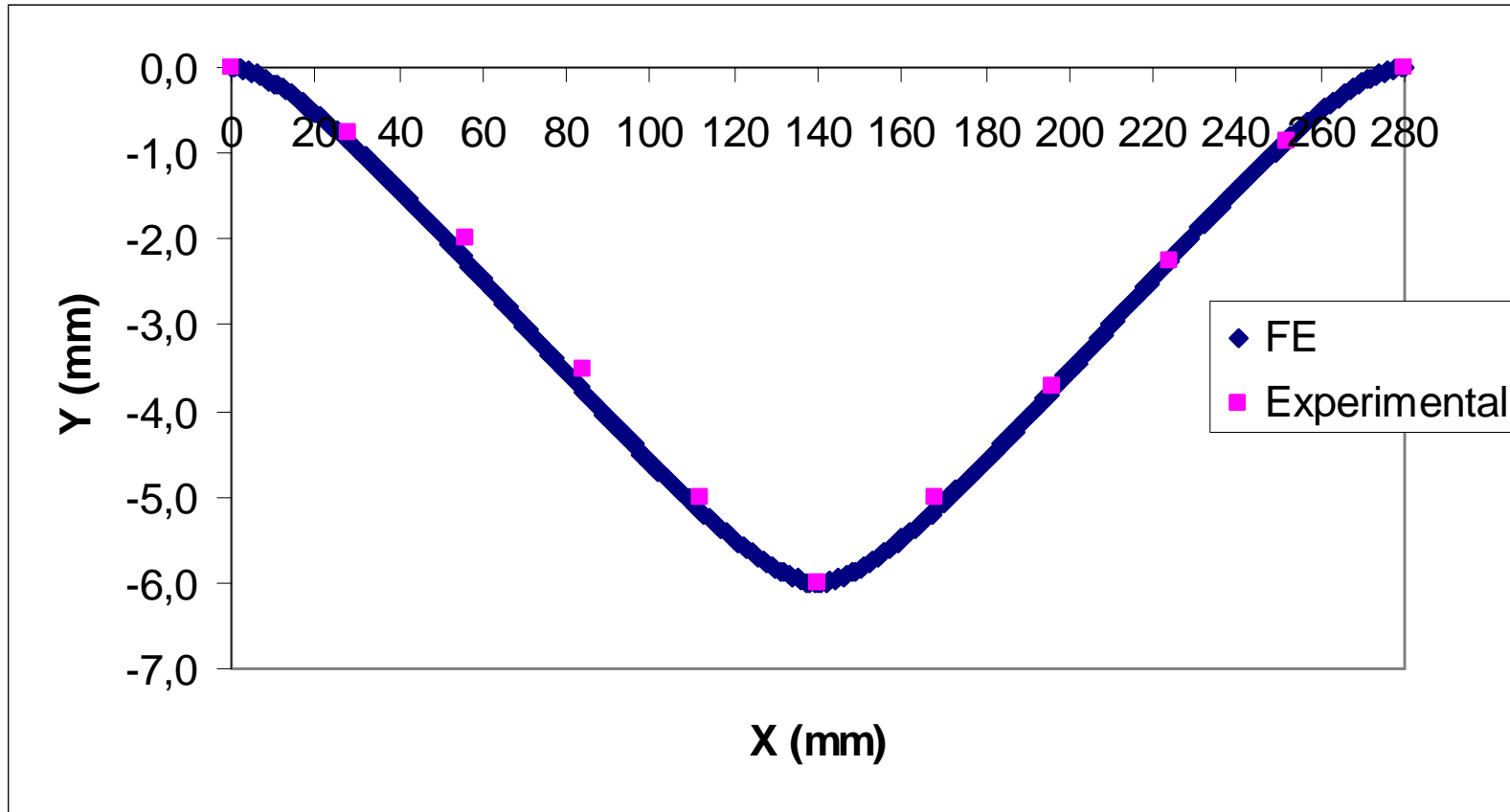
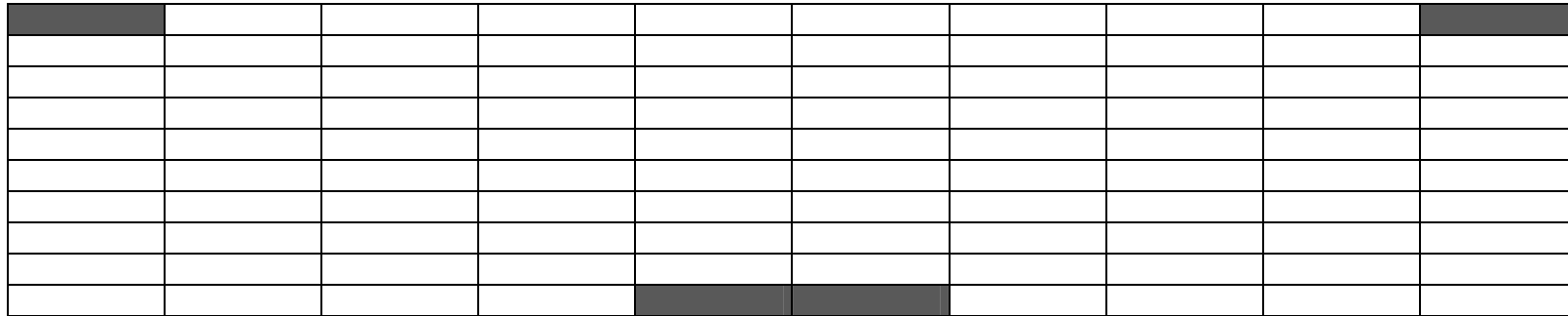
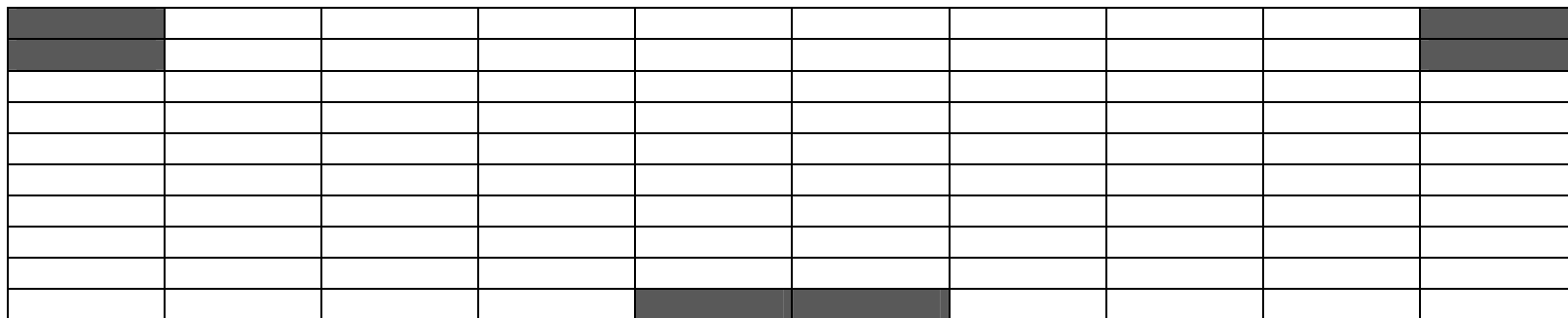


Fig 4.5 (Continue)

(d)



(a)



(b)

Fig. 4.6 Elements Deformed Plastically for mid-deflections at a) 3.5 mm b) 4 mm c) 4.5 mm d) 5 mm e) 5.5 mm
f) 6 mm g) 6.5 mm h) 7 mm

■									■
■									■
■									
				■	■				
				■	■				

(c)

■									■
■									■
■									■
■									■
				■	■				
				■	■				
■									■

(d)

Fig. 4.6 (Continue)

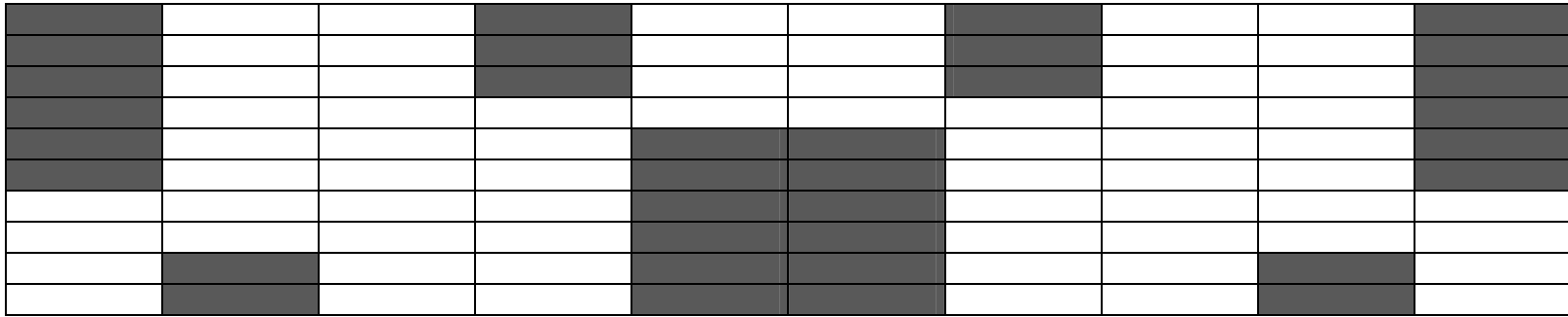
■			■			■			■
■									■
■									■
				■	■				
				■	■				
				■	■				
	■			■	■			■	

(e)

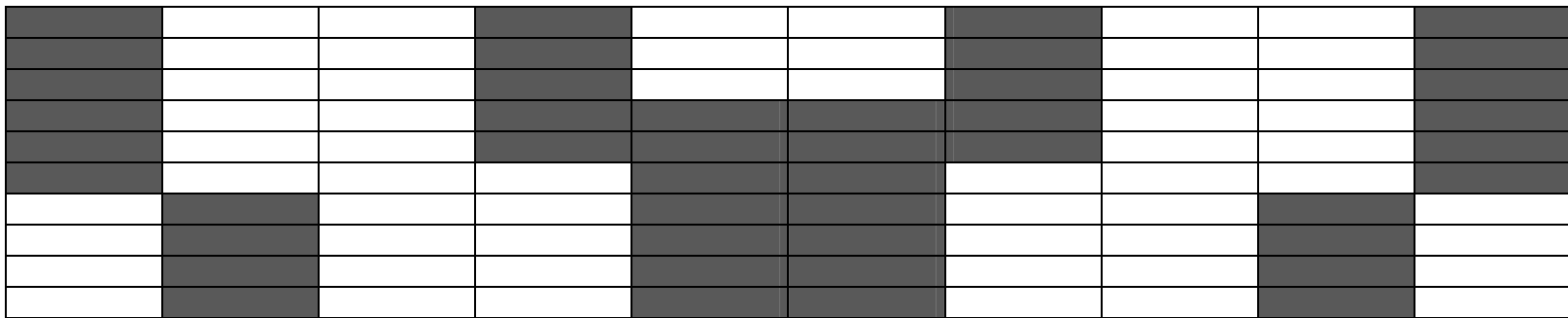
■			■			■			■
■									■
■									■
■									■
				■	■				
				■	■				
				■	■				
	■			■	■			■	

(f)

Fig. 4.6 (Continue)



(g)



(h)

Fig. 4.6 (Continue)

4.3 Discussion of the Results

The Figure 4.2 shows the elastic-plastic deformation for a cantilever specimen. The results are in good agreement with the experimental results. A small difference is observed for the tip deformation which may be attributed to the experimental measurement errors. The deflection measurements may have measurements errors and the measurements taken are not the ones that correspond to each element but only for every twenty eight elements.

The Figure 4.3 shows the plastically deformed elements for the cantilever case where maximum deformation is obtained in the region closest to the fixed end, and the number of the elements deformed plastically increases towards the free end as the load is increased. The stresses of the elements at the fix end are the highest and decreases towards the free end. The elements at the top and bottom surfaces are under the effect of highest stresses compared to the elements in the inner region at the same cross section.

In the Figure 4.5 the deflections of the beam clamped from both ends are given under various loads. The vertical deflection is smaller than the cantilever beam as a result of boundary conditions which make the beam stiffer. In Figure 4.6 the plastically deformed elements and layers are given. The maximum stresses are obtained in the elements that are either in the middle of the beam where the load is applied or at the fix ends. The plastic deformation starts from the bottom layers and expands towards the top layers in the middle of the specimen. The reverse is observed at the fix

ends. An unsymmetrical distribution of plastic elements observed as shown in some figures which can be attributed to numerical approximations and the methodology chosen to show the plastic zones which is described in sections 4.1 and 4.2.

CHAPTER V

CONCLUSION

In this thesis, a finite element is developed for large strain and large deformation elastic-plastic analysis of beams. The two node beam element has three degrees of freedom, two translational and at each node one rotational. The material is isotropic and obeys Von Misses yield criterion. The work hardening characteristics of the material are also included. All nonlinear terms are implemented and Updated Lagrangian formulation is used starting from virtual work principle.

A code is developed and implemented to an elastic plastic finite element program. The outputs of the program are the nodal displacements and the strain and stress values of the elements. From the results of the finite element analyses and experiments following conclusions are obtained:

1. The developed beam element can be applied to model the elastic-plastic large deformations of beams successfully.
2. The element is free from shear locking and has minimum number of nodes.
3. A good agreement is observed between the finite element and the experimental results. The small differences between the results are attributed to the experimentation and approximations in the material properties.

4. The results obtained show that the formulation can be applied to more complicated problems of beam deformation.

For future work, the developed program can be easily adopted to the solution of elastic-plastic three dimensional beam problems. Also another future work could be implementing the formulation to the dynamic problems by adding mass matrices.

REFERENCES

- [1] Timoshenko S.P, *History of Strength of Materials*, McGraw-Hill :New York,1953
- [2] Jennings A, *Int. J.of Mech. Sciences* 1963; 5:99-113.
- [3] Connor JJ, Logcher RD,Chan SC, *J.of Structural Division*, ASCE 1968; 94
- [4] Mallet RH, Marcal P, *J.of Structural Division*,ASCE 1968; 94:2081-2105
- [5] Bathe KJ, Bolourchi S, *Int.J. for Numerical Meth. in Engng* 1979; 14:961
- [6] Conci A, *Journal of Eng. Mechanics*, ASCE 1992; 118:1859-1875.
- [7] S.P. Timoshenko, 'On the correction for shear of the differential equation for transverse vibration of prismatic bars' *Phil. Mag.*, XLI,744-746,1921.Reprinted in 'The Collected Papers of Stephen P. Timoshenko', Mc Graw-Hill, London,1953.
- [8] Reissner E, *Zeitschrift für Angewandte Mathematik und Physik* 1972; 23:795-804.
- [9] Simo JC, *Computer Meth. in Applied Mechanics and Engineering* 1985; 49:55-70

- [10] Simo JC, Vu Quoc L, *Computer Meth. in Applied Mechanics and Engineering* 1986; 58:79-116
- [11] Cardona A and Geradin M, *Int. J. for Numeric. Methods in Engineering* 1988; 26:2403-2438
- [12] Crisfield MA, *Computer Meth. in Applied Mechanics and Engineering* 1990; 81:131-150
- [13] Crivelli LA, *Aerospace Engineering Sciences, Univ. Of Colorado: Boulder*, 1991; 197
- [14] Crivelli LA, Felippa CA, *Int. J. for Numeric. Meth. In Engng* 1993; 36:3647-3673
- [15] M. Schulz and F. C. Filippou, 'Non-linear Spatial Timoshenko Beam Element with Curvature Interpolation', *Int. J. Numer. Meth. Engng* 2001; 50:761-785
- [16] Z. Friedman and Kosmatka J.B, 'An improved two-node Timoshenko beam finite element', *Computers & Structures (ISSN 0045-7949)*, vol. 47, no. 3, p. 473-481. ,05/1993, 1993CoStr.47.473F
- [17] Moshe Eisenberger, 'Derivation of shape functions for an exact 4-D.O.F. Timoshenko beam element' *Communications in Numerical Methods in Engineering* V10, Issue 9 ,P673-681, June 2005

- [18] Seok-Soon Lee, Jeong-Seo Koo and Jin-Min Choi, 'Variational formulation for Timoshenko beam element by separation of deformation mode', *Communications in Numerical Methods in Engineering* V10, Issue 8, P599-610 June 2005
- [19] J.M. Wang, 'Timoshenko Beam-Bending Solutions in Terms of Euler-Bernoulli Solutions', *Journal of Engineering Mechanics* V 121, 6, 763-765 (June 1995)
- [20] E. Yamaguchi, W. Kanok-Nukulchai, M. Hammad and Y. Kubo, 'Simple Degenerate Formulation for Large Displacement Analysis of Beams', *J. Engineering. Mech.* V 125, Issue 10, 1140-1146 (October 1999)
- [21] G. M. Kulikov and S. V. Plotnikova, 'Non-conventional non-linear two-node hybrid stress-strain curved beam elements', *Finite Elements and Design* V40, Issue 11, 1333-1359
- [22] H. Antes, 'Fundamental solution and integral equations for Timoshenko beams', *Computers & Structures*, V81, 6, 383-396
- [23] Moshe Eisenberger, 'An exact high order beam element', *Computers and Structures* V8, 3, 147-152
- [24] R.M. McMeeking and J.R. Rice, 'Finite elements formulations for problems of large elastic-plastic deformation', *Int. J. Solids and Structures*, **11**, 601-616 (1975).

- [25] M. Gotoh, 'A Finite element analysis of general deformation of sheet metals', *Int. J. for Numerical Methods in Engineering*, **8**, 731 - 741 (1974).
- [26] J. C. Nagtegaal, D. M. Parks and J. R. Rice, 'On numerically accurate finite element solutions in the fully plastic range', *Comp. Meths. Appl. Mech. Eng.*, **4**, 153 - 177 (1974).
- [27] J. Backlund and H. Wennerstrom, 'Finite element analysis of Elasto-Plastic shells', *Int. J. for Numerical Methods in Engineering*, **8**, 415-424 (1974).
- [28] J. H. Argyris and M. Kleiber, 'Incremental formulation in nonlinear mechanics and large strain Elasto-Plasticity-Natural approach. Part I', *Comp. Meths. Appl. Mech. Eng.*, **11**, 215 - 247 (1977).
- [29] J. H. Argyris, J. St. Doltsinis and M. Kleiber, 'Incremental formulation in nonlinear mechanics and large strain Elasto-Plasticity-Natural approach. Part II', *Comp. Meths. Appl. Mech. Eng.*, **14**, 259 - 294 (1978).
- [30] J. H. Argyris and J. St. Doltsinis, 'On the large strain inelastic analysis in natural formulation Part I: Quasistatic problems', *Comp. Meths. Appl. Mech. Eng.*, **20**, 213 - 251 (1979).

- [31] J. H. Argyris and M. Kleiber , 'Incremental formulation in nonlinear mechanics and large strain elasto-plasticity - natural approach, Part I', *Comp. Meths. Appl. Mech. Eng.*, **11** , 215 – 247 (1977) .
- [32] J. H. Argyris, J. St. Doltsinis and M. Kleiber , 'Incremental formulation in nonlinear mechanics and large strain elasto-plasticity-natural approach, Part II', *Comp. Meths. Appl. Mech. Eng.*, **14** , 259 – 294 (1978) .
- [33] J. H. Argyris, J. St. Doltsinis, H. Balmer , P.C Dunne, M. Haase, M. Kleiber, G. Malejannakis, H. P Mlejnek, M. Müller, D. W. Scharpf, 'Finite element method the natural approach, Fenomech '78' , *Comp. Meths. Appl. Mech. Eng.*, **17/18** , 1 – 106 (1979) .
- [34] A. Chandra and S. Mukherjee, 'A finite element analysis of metal forming problems with an elastic-viscoplastic material model' , *Int. J. for Numerical Methods in Engineering*, **20** , 1613 – 1628 (1984)
- [35] S. Lu and T. Q. Ye , 'Direct evaluation of singular integrals in elastoplastic analysis by the boundary element method', *Int. J. for Numerical Methods in Engineering*, **32** , 295-311 (1991).
- [36] K. Axelsson and A. Samuelsson, 'Finite element analysis of elastic-plastic materials displaying mixed hardening' , *Int. J. for Numerical Methods in Engineering*, **14** , 211- 225 (1979)

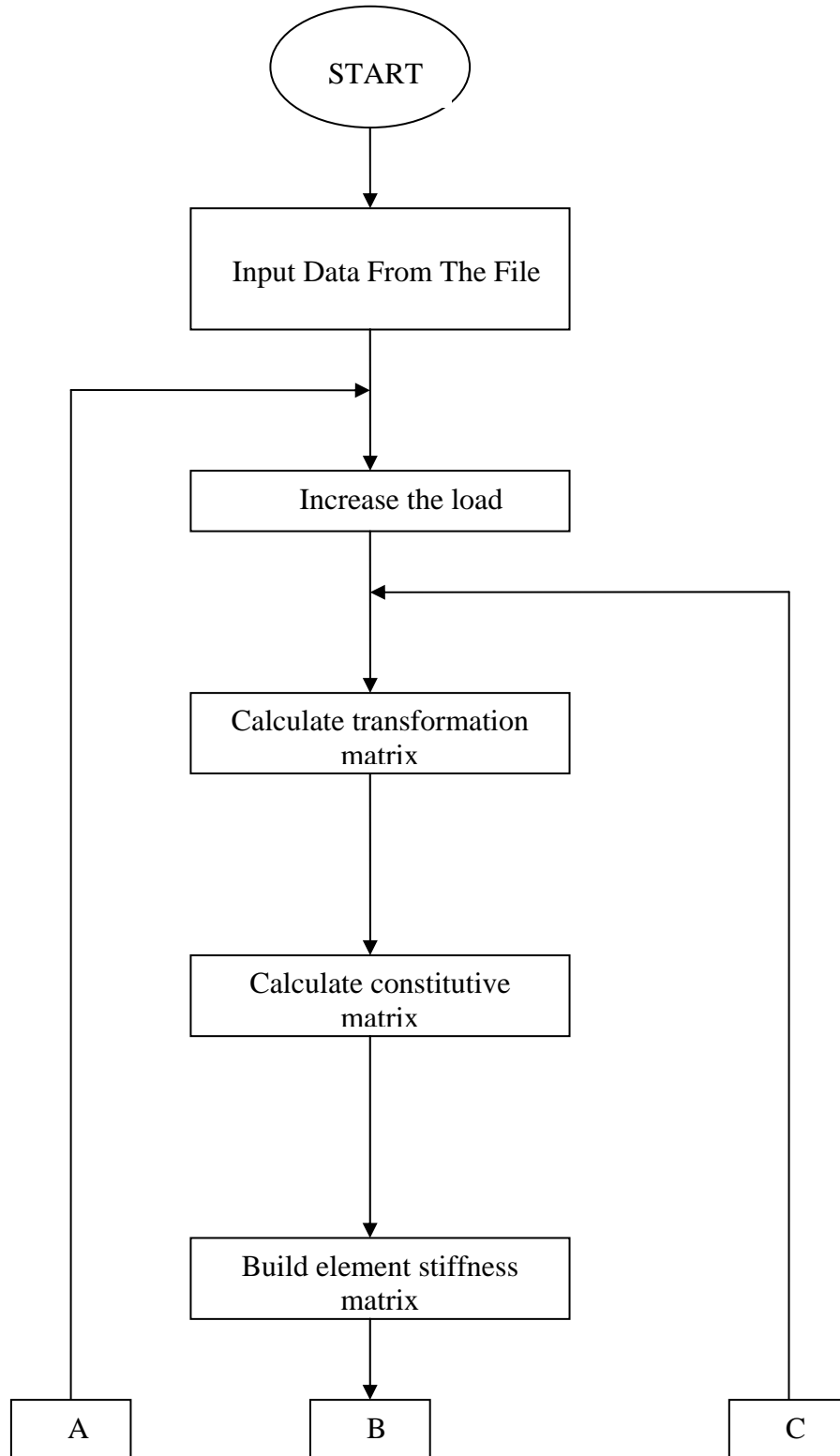
- [37] J. C. Simo, 'A framework for finite strain elastoplasticity based on maximum plastic dissipation and the multiplicative decomposition. PartII: Computational aspect', *Comp. Meths. Appl. Mech. Eng.*, **68** , 1-31 (1988).
- [38] J. C Simo and J. G. Kennedy, R. L. Taylor, 'Complementary mixed finite element formulations for elastoplasticity', *Comp. Meths. Appl. Mech. Eng.*, **74** , 177-206 (1989).
- [39] H. Okada, H.Rajiyah and S.N Atluri,' Some recent development in finite-strain elastoplasticity using the field boundary element', *Computers&Structures* , **30** , 275-288 (1988).
- [40] B. Moran , M. Ortiz and C. F. Shih, 'Formulation of implicit finite element methods for multiplicative finite deformation plasticity', *Int. J. for Numerical Methods in Engineering* , **29** , 438-514 (1990).
- [41] P.Gratacos, P. Montmitonnet, and J. L. Chenot, 'An integration scheme for Prandtl-Reuss elastoplastic constitutive equations', *Int. J. for Numerical Methods in Engineering*, **33**, 943-961 (1992).
- [42] M. Ristinmaa and J. Tryding, 'Exact integration of constitutive equations in elasto-plasticity', *Int. J. for Numerical Methods in Engineering*, **36** , 2525-2544 (1993).

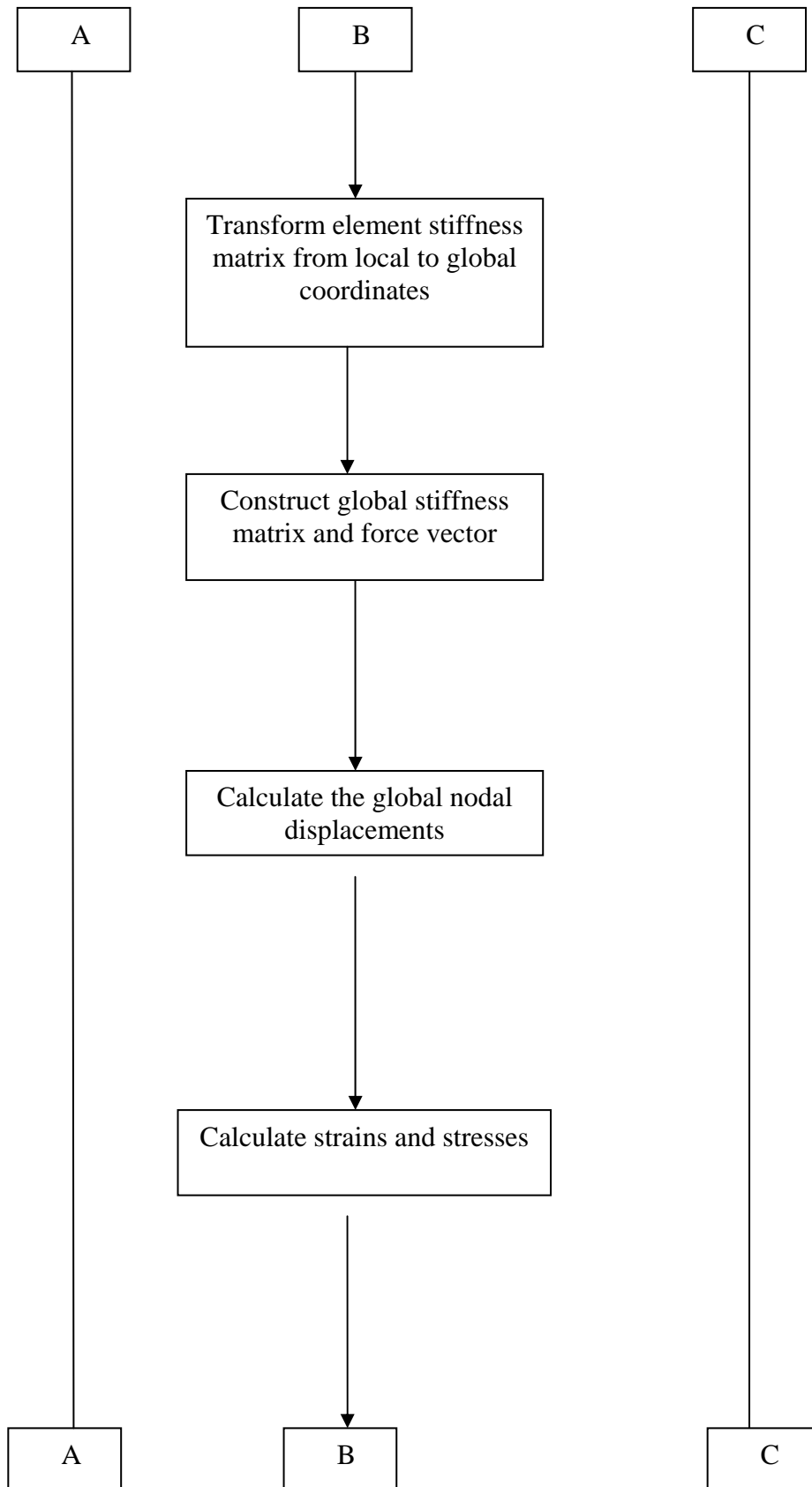
- [43] J. R. Osias and J.L. Swedlow, 'Finite elasto-plastic Deformation-I (Theory and Numerical Examples)', *Int. J. Solids Structures*, **10**, 321-339 (1974).
- [44] K. J. Bathe and H. Özdemir, 'Elastic-plastic large deformation static and dynamic analysis', *Computers & Structures*, **6**, 81-92 (1976).
- [45] S. Caddemi and J. B. Martin, 'Convergence of the Newton – Raphson algorithm in elastic – plastic incremental analysis', *Int. J. for Numerical Methods in Engineering*, **31**, 177 – 191 (1991).
- [46] R. Borst , H. B. Mühlhaus , 'Gradient – dependent plasticity: formulation and algorithmic aspect', *Int. J. for Numerical methods in Engineering*, **35**, 521- 539 (1992).
- [47] C. Miehe , 'On the representation of Prandtl – Reuss tensors within the framework of multiplicative elastoplasticity', *Int. J. of Plasticity*, **10**, 609-621 (1994).
- [48] L. Shu and F. T. Hua , 'An efficient method for elastic-plastic analysis of destructive structures', *Computer & Structures*, **59**, 911-914 (1996).
- [49] A. Turgut , 'An Elastic – Plastic Shell Finite Element', Msc. Thesis , Middle East Technical University, Ankara (1997).

- [50] H. Darendeliler, ' Computer Aided Deformation Analysis of Deep Drawing Process ', Ph. D. Thesis , Middle East Technical University, Ankara(1991).
- [51] K. J. Bathe, Finite Element Procedures, Prentice-Hall , Inc .,New Jersey (1996).
- [52] AC. Eringen , Nonlinear Theory of Continous Media, McGrew-Hill Book Company, Inc., New York (1962).
- [53] L. E Malvern, Introduction to the Mechanics of a Continous Medium, Prentice-Hall, Inc., New Jersey (1969).
- [54] Y.Yamada and N. Yoshimura, ' Plastic Stres-Strain Matrix and Its Application for the Solution of Elastic Plastic Problems by the Finite Element Method', *Int.J. Mech. Sci.* , **10** , 343-354 (1968).

APPENDIX A

FLOWCHART OF THE PROGRAM





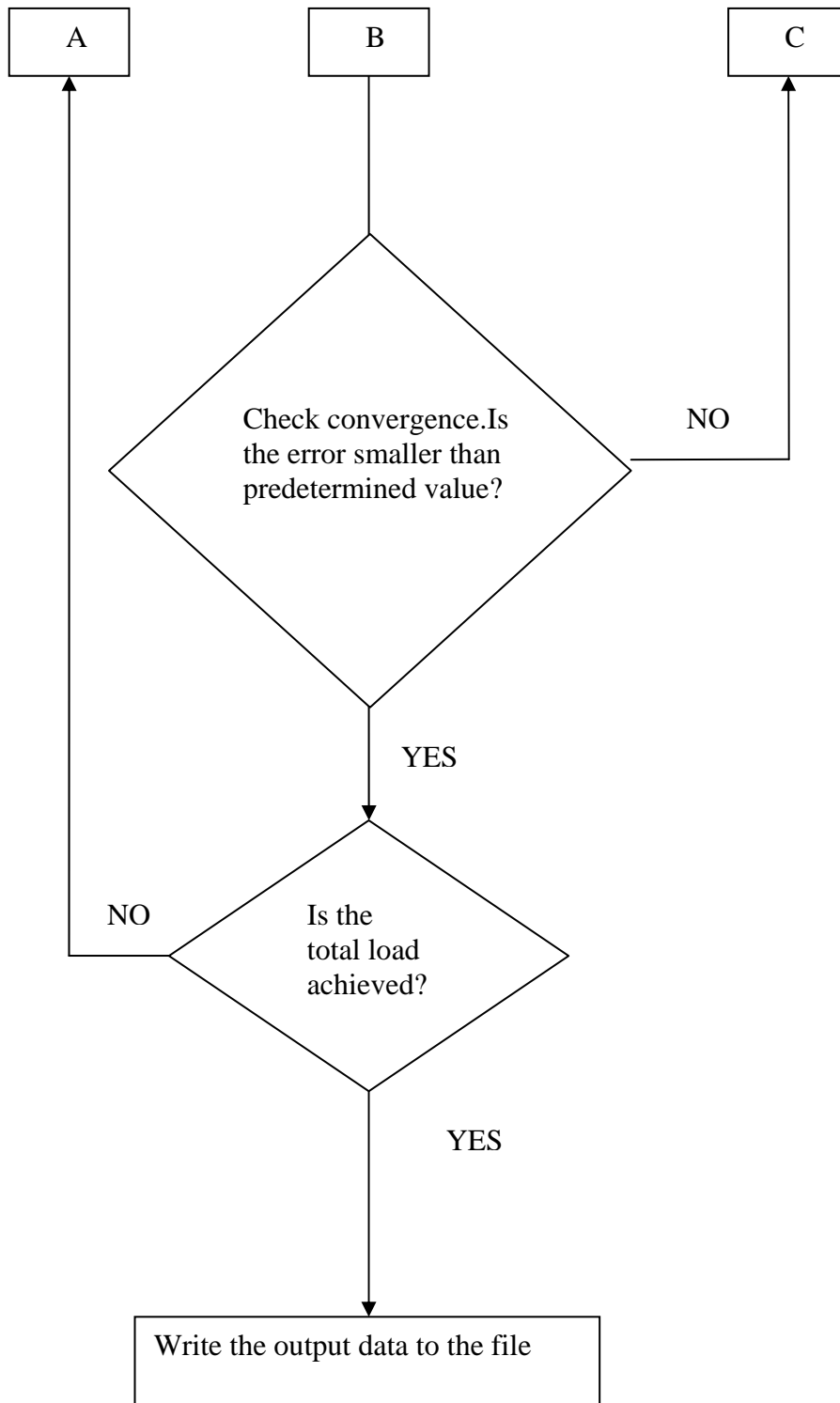




Figure B1. The Stress-Strain Curve of the 2,68 mm thick Test Specimen